Masterarbeit

The function of TSC2 in macrophages in regard to tissue homeostasis and metabolism

Verfasserin

Monika Linke BSc

angestrebter akademischer Grad

Master of Science (MSc)

Wien, 2014

Studienkennzahl	A 066 830
Studienrichtung	Masterstudium Molekulare Mikrobiologie und Immunbiologie
Betreuer	Univ.-Prof. Mag. Dr. Pavel Kovarik

Contents

1. Introduction

1.1 Macrophages

1.1.1 Origin and heterogeneity

First described due to their phagocytic nature by Eli Mechnitoff, macrophages represent a heterogeneous subset of innate immune cells that participate in a broad variety of biological processes. Already in 1925 Sabin *et al.* proposed that monocytes are the precursor of macrophages[1]. A concept that was later on termed the mononuclear phagocyte system and was officially accepted to represent the origin of macrophages at a conference in 1969. Accordingly, heamatopoietic progenitors gradually develop into monocytes, which after being released into the bloodstream seed into various tissues where they mature as macrophages. These are then gradually replenished by bone marrow derived monocytes[2]. However this linear model was in conflict with several phenomena, for example local macrophage proliferation or the presence of fetal macrophages, prior heamatopoiesis[3]. That the first macrophages lack a monocytic progenitor and arise from the yolk sac was already suspected in the 1980's and confirmed by recent fate mapping studies and gene expression profiles. After vascularisation the fetal liver provides the niche for definitive hematopoiesis, which later on shifts to the bone marrow[4,5,6,7,8]

The development and maintenance of macrophages are dependent on growth factors such as macrophage-colony stimulating factor (M-CSF), granulocyte/ macrophage-colony stimulating factor (GM-CSF) or IL-34[9,10]. Important insights have been gained from the comparison of two mouse models, namely $CSF1^{op/op}$ and $CSFR1^{-/-}$ mice (the gene encoding for M-CSF and its cognate receptor respectively)[11,12]. Both mouse models show similar deficiencies, the typical osteopetrotic (bone thickening) phenotype as well as the lack of the majority of macrophage populations. However in $CSFR1^{-/-}$ an additional deficiency of microglia and Langerhans cells was observed, indicating an alternative ligand for macrophage-colony stimulating factor receptor (M-CSFR), which was indeed identified as IL-34[11,12,13,14,9,10]. In contrast, decelopment of the population of alveolar macrophages from fetal liver progenitors has been shown to be GM-CSF dependent[15].

Interestingly, prenatal yolk sac-derived macrophages seem to provide most of

the tissue-resident macrophages ($F4/80^{high}$), which are able to maintain themselves, while bone marrow-derived monocytes feed into $F4/80^{low}$ macrophage and dentritic cell populations[6,9,10]. Monocytes are classically divided into circulating ($Ly6C^{-}$) and inflammatory ($Ly6C^{+}$) monocytes[16,17]. Commonly used macrophage markers include F4/80, CD11b (or MAC-1) and CD68, but in specific settings also CD11c (which is also a classical dendritic cell marker), MAC-2 (galectin-3) and many others, that are not only helpful, but often necessary to identify specific subpopulations[9]. The observed heterogeneity of macrophage populations is only partially explainable by separate origins; an important hallmark of macrophage biology is their high plasticity. Macrophage functionality can be shaped by their niche, which led to the concept of M1 and M2 macrophages[18]. Although this represents a simplified view, it highlights the capacity of macrophages to adapt their function according to environmental clues.

1.1.2 Functions in immunity and homeostasis

Macrophages are found in most tissues of the body and they are well known for their role as immune sentinels. Prominent representatives are alveolar macrophages (lung), red pulp macrophages (spleen), microglia (brain) and kupffer cells (liver), osteoclasts (bone), to give a few examples.

This broad distribution puts them in an excellent place to rapidly sense mechanical insult or microbial stimuli. Macrophages express multiple of receptors that recognize pathogen-associated molecular patterns (PAMPs) or danger-associated molecular patterns (DAMPs)[19,20]. These are commonly known as pattern recognition receptors (PRRs) and include toll-like receptors (TLRs), but also nod-like receptors (NLRs) and rig-I-like receptors (RLRs). Furthermore macrophages express a vast array of scavenger receptors, which are essential in their role as phagocytes as they support phagocytosis and endocytosis[19,21,22]. Upon tissue injury macrophages (and other tissue resident cells) launch influx of neutrophils, monocytes (as a source of inflammatory macrophages) and leukocytes into affected tissues. Microbial-activated inflammatory macrophages in turn secrete high amounts pro-inflammatory cytokines, such as TNFα, IL-1, promote oxidative processes and IL-12 and IL-23 production boosts T_H1 and T_H17 mediated response. Additionally, anti-microbial molecules, such as nitrite oxide are produced, thereby not only damaging the invading organism, but also the host[17,10].

The importance of macrophages in immunity in inflammation is well recognized, however, they also play an important role in homeostatic settings. They take part in the resolution of inflammation by facilitating phagocytosis of apoptotic cells and debris, which suppresses inflammation in a self-antigen mediated manner. Anti-inflammatory feedback mechanism also include the production of IL-10, which promotes T_{Reg} expansion[17,9,10]. Macrophages are also implicated in tissue patterning and branching morphogenesis, for example of the mammary gland and pancreas[10,23]. Importantly, tissue remodelling also plays an prominent role in maintenance of stem cell niches. For example $CSF1^{op/op}$ mice display not only an osteopetrotic phenotype, but compromised hematopoiesis in

the bone as they lack cavity sculpturing by osteoclasts[10,23]. Osteoclast shape the bone niche, while bone marrow-resident macrophages (central macrophage) provide the platform for erythropoiesis. Multiple pro-erythrocytes of various stages have been found to "sit" on the central macrophage, that is said to have nourishing functions, but also phagocytoses the expelled nucleus[24,25]. Additionally, red pulp macrophages of the spleen phagocytose aged erythrocytes and facilitate haeme recycling[26,25]. Therefore, macrophages also are not only essential in the erythroid life-cycle but also for the maintenance of iron homeostasis illustrating their role in metabolism and tissue integrity.

1.2 The mTOR pathway

1.2.1 Rapamycin and mTOR

Mechanistic (former mammalian) target of rapamycin (mTOR) is an evolutionary conserved serine/threonine kinase, that forms the core of two signaling platforms in the cell, called mTOR complex 1 (mTORC1) and mTOR complex 2 (mTORC2). Initially mTOR (or more specifically mTORC1) was identified to be the target of the macrolide product rapamycin, whereas mTORC2 activity is not directly blocked by rapalogues[27,28,29,30].

Rapamycin was found to be a highly specific inhibitor and was introduced as an immunosuppressant and further as a cancer treatment drug[30]. When bound to FK506-binding protein of 12kDa (FKBP12) rapamycin suppresses kinase activity by physical interaction with mTORC1[30,31]. However this process was found to be only partially effective, while ATP-competetive inhibitors (such as torin) block both mTORC1 and mTORC2 activities[30].

Importantly, both complexes are sensitive to phosphatidylinositol 3-kinase (PI3K) activity and while mTORC2 functions upstream of Akt, mTORC1 resides downstream of the PI3K-Akt-tuberous sclerosis complex (TSC) axis, which might be viewed as the classical mTOR pathway.

1.2.2 mTORC1/2 components

mTORC1 and mTORC2 share not only the catalytic subunit mTOR, but also mammalian lethal with sec-13 protein 8 (mLST8) which seems to be essential mainly for mTORC2 activity, the scaffolding tel two interacting protein (Tti)/tel2 complex, as well as their common inhibitor DEP domain containing mTOR- interacting protein (DEPTOR)[32,33,34]. In addition, mTORC1 comprises of regulatory-associated protein of mTOR (Raptor) and proline-rich akt substrate of 40 kDa (PRAS40). Raptor, besides providing scaffolding and localizing properties for mTORC1, recruits and binds substrates, while association with PRAS40 negatively regulates mTORC1 function[31,35,36]. Rapamycin-insensitive companion of mTOR (Rictor) represents the mTORC2 counterpart to mTORC1s Raptor, and its two other complex specific subunits — stress-activated protein kinase-interacting protein (mSin1) and protein observed with

rictor 1 and 2 (Protor1/2) — positively mediate mTORC2 function[32,37,38].

1.2.3 mTORC1 activation and function

As mentioned above, both complexes are downstream of PI3K, which is sensitive to a variety of stimuli, whereas in an immunologic setting it is important to mention cytokine receptors, co-stimulatory molecules and TLRs[39,40]. The prototype of PI3K activation, however, is by growth factors, such as insulin and insulin-like growth factor (IGF), binding to their cognate cell surface receptor. Thereupon insulin substrate receptor 1 (IRS1) is recruited to the plasma membrane-bound receptor and activates PI3K. PI3K (or class IA PI3K; hereafter referred to as PI3K) comprises of a catalytic p110 and a regulatory p85 subunit, and converts phosphatidylinositol-4,5-biphosphate (PIP2) to PI-3,4,5-P (PIP3)[27,41,39].

PIP3 acts as a second messenger, which not only recruits phosphoinositide-dependant kinase 1 (PDK1) and Akt to the cell membrane, but also results in the activation of mTORC2[42,43]. PDK1 and mTORC2 phosphorylate Akt at T308 and S473 respectively, to provide full activation of Akt[43]. Thereupon Akt phosphorylates and inhibits TSC, the main negative regulator of mTORC1 signaling[44].

TSC comprises of two essential subunits: hamartin (TSC1) and tuberin (TSC2). While TSC1 is thought to mainly stabilize the complex, TSC2 functions as a GTPase activating protein (GAP) for the small GTPase ras homolog enriched in brain (Rheb), a potent activator of mTORC1[45,46]. Additionally the supressive function of TSC is also relieved due to other inputs, for example the Ras-extracellular signal-regulated kinase (ERK) pathway and ribosomal S6 kinase (RSK), or as recently shown in human monocytes p38α-MAPK activated protein kinase 2 (MK2)-mediated phosphorylation[47,48,49]. However, phosphorylations not only releases the inhibitory function of TSC, as glycogen synthase kinase 3β (GSK3), AMP-dependent protein kinase (AMPK) or Redd strengthen the inhibitory function of TSC thereby[50,51,52]. Disruption of TSC thus renders its GAP activity on Rheb, which in its GTP–loaded state facilitates the phosphorylation and activation of mTORC1. As TSC incorporates these vast amount of inputs, (like growth factor, wnt and MAPK signaling, stress as well as the cellular energy status) it might be viewed as the switchboard operator of mTORC1 activity.

The functional output of mTORC1 signaling is often accessed by the phosphorylation levels of its best described downstream mediators eukaryotic translation initiation factor 4E (eIF-4E) binding protein 1 (4E-BP1) and ribosomal protein S6 kinase 1 (S6K1) (and/or its following target S6). Phosphorylated 4E-BP1 can no longer bind to eIF-4E, thus allowing it to participate in cap-dependent mRNA translation while S6K1 promotes mRNA biogenesis and translational initiation[53]. Of note, strong S6K1 activation supports the activation of a negative feedback loop to IRS1. Accordingly S6K1 dependent phosphorylation subjects IRS1 to proteasomal degradation, thereby blocking the action of PI3K[54,55].

However, the role of mTORC1 reaches far beyond protein synthesis. For

example, lipid synthesis is initiated through the combined effort of activating sterol regulatory element-binding proteins (SREBPs) and retaining their cognate inhibitor Lipin1 in the cytoplasm[56,57]. Also yin-yang 1 (YY1) is a substrate of mTORC1 and when phoshorylated, YY1 forms a complex with peroxisom-proliferator-activated receptor coactivator-1α (PGC-1α) and promotes mitochondrial biogenesis[58]. Cellular energy status (ATP-AMP ratio) is monitored via AMPK. While sufficient ATP renders AMPK inactive, rising cellular AMP levels activate AMPK[59,56,60]. AMPK counteracts mTORC1 signaling on several levels. It stabilizes the inhibitory function of TSC, can block mTORC1 signaling through phosphorylation of raptor and also promote autophagy initiation directly[60]. Furthermore, mTORC1 activity is directly related to amino acid availability. Interestingly amino acid stimulation induces the translocation of the signaling complex to the lysosomal surface, where it subsequently can be activated by Rheb[61]. Althought the direct sensor of amino acids is still elusive, this mechanism requires the ras-related (Rag) GTPases, the pentameric Ragulator complex and the vacuolar H^+- ATPase (v-ATPase)[61,62,63,64]. Besides promoting cell growth by the induction of anabolic processes, mTORC1 also supports net cell-mass accumulation by the suppression of autophagy, and has recently been shown to modulate transcription factor EB (TFEB), a "master regulator" of lysosomal biogenesis. mTORC1 phosphorylation supresses the ULK1/Atg13/FIP200 (unc-51-like kinase 1/autophagy-related gene 13/focal adhesion kinase family-interacting protein of 200kDa) complex, which plays an important role in the initiation of autophagy[65,66]. TFEB promotes lysosomal and autophagy gene transcription, and phosphorylation by mTORC1 apparently promotes its retention in the cytoplasm[67,68,69,70,71].

Collectively, the mTOR–pathway integrates both environmental cues, such as growth factors and nutrient availability, as well as the cellular energy status into cellular fate. These signals exert their effect on various levels of the pathway and it is still questionable up to which extent one signal overrules another. mTORC1 definitely plays a central role in orchestrating this vast amount of extra- and intracellular signals and intriguingly, it does that in a cell-type specific manner. In the immune system for example, mTORC1 promotes the clonal expansion of adaptive immune cells, while it inhibits pro-inflammatory innate immune responses[39,40].

1.3 Lysosomes

1.3.1 Structure and function

In the 1950ies Christian de Duve and his laboratory studied carbohydrate metabolism and the action of insulin on the liver, by accessing subcellular fractionation to examine enzyme localization and further enzyme activity[72]. As a byproduct of their research they stumbled over a 'bizarre' activity pattern of acid phosphatase: In fresh homogenates the enzyme displayed activity latency, which could be restored either by harsher homogenizing techniques or simply

by storage of the fractions in the refrigerator for a couple of days[73,72]. Further de Duve and his colleagues identified 5 hydrolases with acidic pH optima in 'membrane bound pockets'. As their functional targets were broadly varying, they concluded that these granules represented a digestive compartment of the cell, hence termed lysosomes (greek for 'digestive body')[74].

Today lysosomes are not only recognized for their role in cellular clearance and recycling, but also for their function in cellular homeostasis, plasma membrane repair, bone and tissue remodeling, cell signaling, immune response and cell death[75,76,77]. Lysosomes can be identified by their most common membrane proteins: lysosome-associated membrane protein 1 (LAMP1), lysosome-associated membrane protein 2 (LAMP2), lysosomal integral membrane protein 2 (LIMP2) and CD63/lysosomal integral membrane protein 1 (LIMP1). They are known to appear mainly as electron dense organelles of globular or tubular shape and a commonly used visualizing technique includes staining with pH sensitive dyes, or tracing of labeled substrates that target the lysosome[76,77,78].

As already stated by de Duve, lysosomes degrade a multitude of structurally diverse macromolecules and their monomeric constituents, provide valuable building blocks for the cell. These building blocks are then translocated retrograde into the cytoplasm utilizing various transporters, or are targeted to the cell surface for exocytosis[78,79].

The major players of metabolite breakdown are over 50 lysosmal hydrolases (or acid hydrolases) that are present within the lysosomal lumen, all essential to maintain the degratory capacity of cells[75,78,77]. A single lipidbilayer provides the barrier between the highly acidic lumen (pH 4,5-5) and the cytoplasm. The lysosomal pH is obtained and maintained by the action of the v-ATPase, a transmembrane multimeric complex that has a similar structure as the the mitochondrial F-ATPase[80,81,82]. However the F-ATPase functions mainly as an ATP-synthase coupled to the respiration chain, though it is able to work in both directions (synthesize or hydrolyse ATP). *In vivo* the v-ATPase seems to work only in the hydrolytic direction, whereas its main function is to produce an acidic pH[82]. It utilizes metabolic energy to pump protons against the electrochemical gradient, thereby acidifying the lysosomal interior[83,81,82]. The v-ATPase is found along both the endocytic and exocytic compartments, whereas the pH gradually drops on route to the lysosome[81,82]. Within the lysosome the acidic pH serves several functions: it not only favors the degradation of macromolecules in general, but also induces structural changes of lysosomal proteins, thus promoting enzyme activity[76,82,84]

The destructive potential of lysosomes raises the question how self-degradation of the lysosomal membrane as well as its hydrolases is prevented and lysosomal integrity maintained. Purified lysosomes are readily degraded following ingestion by Kupffer cells, indicating that the inner leaflet of the membrane is actively protected from degradation[85]. Images obtained with transmission electron microscopy show an electron translucent halo covering the inner perimeter of the lysosome that is composed out of carbohydrate moieties[86]. Glycoproteins are found to be more resistant to proteolysis in general and lysomal membrane proteins are heavily glycosylated on their luminal domain[87,88,89]. Therefore,

Granger *et al.* estimated that their high frequency within the lysomal membrane is sufficient to form a continuous carbohydrate coat on its inner perimeter, also known as glycocalyx[89]. Although the glycocalyx lining is still often referred to represent a protective coat of the inner lysosomal membran, Kundra *et al.* showed that it indeed only prevents degradation of a subset of lysosomal membrane proteins[90]. As a general inhibition of glycosilation leads to major cellular abnormalities (the most obvious is the sorting process in golgi), they fed cells with endoglycosidase H. Though cleavage of glycans results in rapid degradation of LAMP1 and LAMP2, no changes in lysosomal integrity are observed (curiously LIMP2 still seemed resistant to degradation)[90].

The impact of dysfunctioning lysosomes is reflected in the occurrence of over 50 lysosomal storage diseases (LSDs). LSDs are inherited diseases with an approximate prevalence of 1 in 8000 births[84,91]. While the causes for LSDs are heterogeneous — failure of enzyme function or delivery, defective traveling, fusion, export or acidification – they result in storage material accumulation and ultimately render lysosomes inoperative. Consequently, degradation of former unaffected substrates is also compromised[84,91,92,75]. The heterogenity of LSDs complicates therapeutic approaches, whereas the most common is the so called enzyme replacement therapy. In this aspect it is of interest to find alternative therapeutic approaches, whereas TFEB has been named as a possible target multiple times[84,91,92].

1.3.2 Routes to the lysosome

Substrates for degradation, but also lysosomal constituents, can reach the lysosome by various routes. External material is ingested by endocytic pathways, while damaged or unnecessary cellular organelles and proteins are sequestered by autophagy.

Endocytosis describes processes where extracellular material is subject to membrane invagination, whereas a multitude of different mechanisms are described in the literature[93,94,95]. Vesicles in the µm scale are established during phagocytosis and macropinocytosis, while small invaginations of 100 to 200nm in diameter are formed due to various mechanisms[95]. These small structures are often referred to as the classical endocytic pathway, and the best described mechanism by far is clathrin-mediated endocytosis. However other "coat" structures, such as caveolin or also uncoated vesicles are becoming increasingly recognized[93,94,95].

Interestingly, specific uptake mechanisms seem to integrate the cellular environment into cell biological decisions. For example, low epidermal growth factor (EGF) concentrations induce activated receptor internalization, mostly by clathrin-mediated endocytosis. Subsequently, the receptor is recycled to the plasma membrane, presumable to continue participating in signaling. On the other hand, high EGF concentrations lead to receptor ubiquitilation, clathrin-independent endocytosis and receptor degradation[96,97]. Another example couples low concentrations of platlet derived growth factor (PDGF) to clathrin-mediated endocytosis and induction of cell migration. However, at high dosage

of PDGF, its receptor is internalized via caveolin, subjected to degradation, and a signaling program that supports cell proliferation is induced [98]. Thus besides playing a very obvious role in cellular nutrition, endocytosis functions in host immunity not only due to its cleansing nature, but in regulating certain signaling circuitries.

Extracellular substrates are first targeted to early endosomes (EEs), then routed via late late endosomes (LEs) to the lysosome. Receptor-bound cargo either dissociates due to the slight acidic environment of the EE, or cargo and receptor go down the same road. For example, the low-density lipoprotein receptors (LDL-Rs) are re-targeted to the plasma membrane after cargo dissociation to be recycled [99]. In general these compartments can be distinguished according to their surface markers, their localization, as well as their appearance. EEs are often identified via early endosome antigen 1 (EEA1) and ras-related in brain 5 (Rab5), they are electron-light membrane compartments, of both tubular and spherical shape and are mostly found in close proximity to the cell surface [76,84,78,77]. During the transition from EEs to LEs cargo concentrates in progressively fewer and larger endosomes that move to the juxtanucleare region. This process is accompanied by an increase of the small GTPase ras-related in brain 7 (Rab7) and loss of Rab5 [100]. Thus LEs are less electron translucent and although they appear mostly as spheres, their interior is broadly varying. They may be filled with membrane worles (membrane sheets) or small vacuoles (then termed multi vesicular body (MVB)) and are identified for example via Rab7, but also lysosomal markers. The most reliable markers for the differentiation of LEs and lysosomes is however, that lysosomes lack mannose-6-phosphate receptors (M6PRs). M6PRs binds to most soluble lysosomal enzymes in the trans-Golgi network, which are subsequently released due to the acidic environment in endosomes, whereafter the receptors are cycled back to the golgi [76,84,78,77]. Alternative sorting mechanisms include sortilin and LIMP2, which have been shown to be responsible for the delivery of distinct hydrolases [101,102].

Importantly, the M6PR route might also lead to the cell surface and from there on to the lysosome, which forms the basis for enzyme replacement therapy in LSDs. Just like lysosomal hydrolases, lysosomal membrane proteins are either transported via an extra- or intracellular route, but they are all delivered by the LEs to the lysosome, which explains the similarity of their markers [76,84,78,77].

The complexity of the endosomal pathway is enormous, as it can not be considered to be a 'one-way street'. At each intermediate stage recycling events are taking place and and cargo might be transmitted by vesicular carrier transport or via tubular connections. Additionally, multiple fission and fusion events take place, whereas the fusion may be permanent or short and transient. Luzio *et al.* fittingly described the processes as a constant molecular and structural remodeling, due to gradual membrane and content exchange [76].

2. Results

2.1 TSC2 deletion in BMDMs induces strong activation of mTORC1

To address the role of TSC2 in macrophage function, we crossed mice harboring loxP flanked TSC2[103] ($TSC2^{fl/fl}$) and mice that express the Cre recombinase under the control of the lysosozym M (LysM) promoter[104] ($LysM^{cre/cre}$). Their respective offspring ($LysM^{cre/cre}$ $TSC2^{fl/fl}$), will hereafter be referred to as $TSC2^{\Delta M}$, as their macrophages (and granulocytes) should be conditionally depleted of TSC2. As controls $TSC2^{fl/fl}$ bone marrow derived macrophages (BMDMs) or mice were used throughout the study.

To determine the functionality of the knock-out, bone marrow (BM) was differentiated *in vitro* into BMDMs as outlined in the Materials & Methods. Thereafter cells were cultivated o/n in starvation media. Thus BMDMs were not only deprived of M-CSF (which promotes macrophage differentiation and proliferation) but were also exposed to reduced serum concentration, to minimize nutrient-mediated mTORC1 activation. Whole cell lysates, analyzed by western blot, confirmed that TSC2 is efficiently knocked out in $TSC2^{\Delta M}$ BMDMs after the differentiation process (Fig.1). As expected, the loss of TSC2 induced strong activation of mTORC1, as even in the non-stimulated control its downstream effectors S6 and 4E-BP1 were highly phosphorylated (hyperphosphorylation of 4E-BP1 can easily be seen due to its upward shift in the SDS-page, thus representing the highest detected band).

Interestingly, even with different TLR stimulants — LPS and Poly(I:C), which represent ligands for TLR4 and TLR3, respectively — the floxed control never reached the basal phosphorylation level of S6 and 4E-BP1 observed in TSC2 knock-outs. Also, a reduction of Akt phosphorylation was seen in $TSC2^{\Delta M}$ BMDMs, both in the medium control as well as in the TLR stimulated samples. This indicates the induction of the negative feedback-loop via S6K1 – IRS1[54,55] and therefore represents an additional sign of constitutive mTORC1 signaling.

In summary, $TSC2^{\Delta M}$ BMDMs efficiently depleted TSC2 during their differentiation, displayed highly elevated mTORC1 activity and represent an excellent tool to study the effects of mTORC1 signaling in murine macrophages.

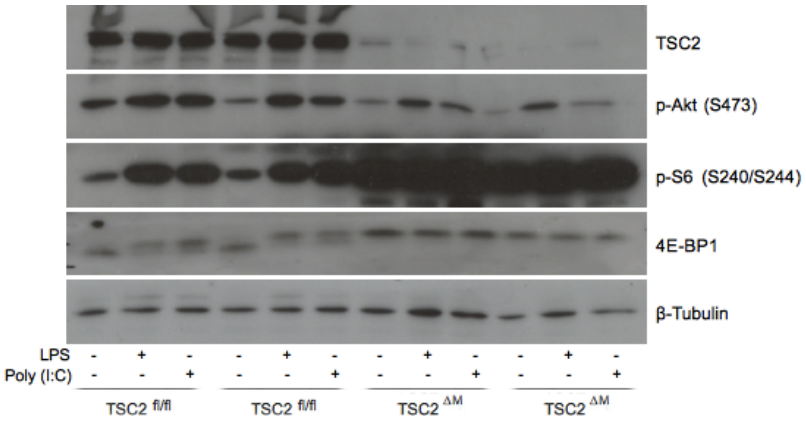

Figure 1: **Differentiation induces loss of TSC2 in TSC2$^{\Delta M}$ BMDMs** On day 7 BMDMs were seeded in starvation medium o/n, stimulated 3h with either 100ng/ml LPS, 50μg/ml Poly(I:C), or were left unstimulated. Cellular lysates were subjected to western blot and probed with the indicated antibodies.

2.2 Cellular morphology is profoundly altered in TSC2$^{\Delta M}$ BMDMs

The phenotype of TSC2$^{\Delta M}$ macrophages was unusually round in comparison to their floxed counterpart (Fig.2a). The lack of TSC2 enhanced the size of BMDMs as shown by Casy measurement and flow cytometry (Fig.2b&c). Besides an increased forward scatter, we also observed a pronounced upward shift in the side scatter. As mTORC1 is known to be a master-regulator of cell growth[51,29,27] the increase in cell size might not be surprising, however the altered side scatter suggested a more substantial change in cellular morphology. Electron microscopy showed that the lack of TSC2 resulted in a multitude of electrone dense organelles (Fig.2d). Additionally, similar dark tubular structures in close proximity of the nucleus were visible. The mentioned organelles were also present in growing autophagic structures, but no closed autophagic vacuole was observed in any of the examined pictures. An irregular mitochondrial structure was also observed in TSC2$^{\Delta M}$ BMDMs (Fig.2d). mTORC1 has been reported to promote mitochondrial biogenesis[58,56,60], however, the lack of TSC2 seemingly introduced highly irregular features of the lamellae.

Thus TSC2 depletion not only increased cell size, but grossly changed macrophage phenotype to a round, highly granular state. Granules were observed as electron dense organelles and the mentioned structures were apparently subjected to autophagy, indicating that their cellular function was perturbed. Additionally, an occasional altered mitochondrial structure, that was not observed in TSC2$^{fl/fl}$ BMDMs, was a prominent feature in TSC2$^{\Delta M}$ BMDMs.

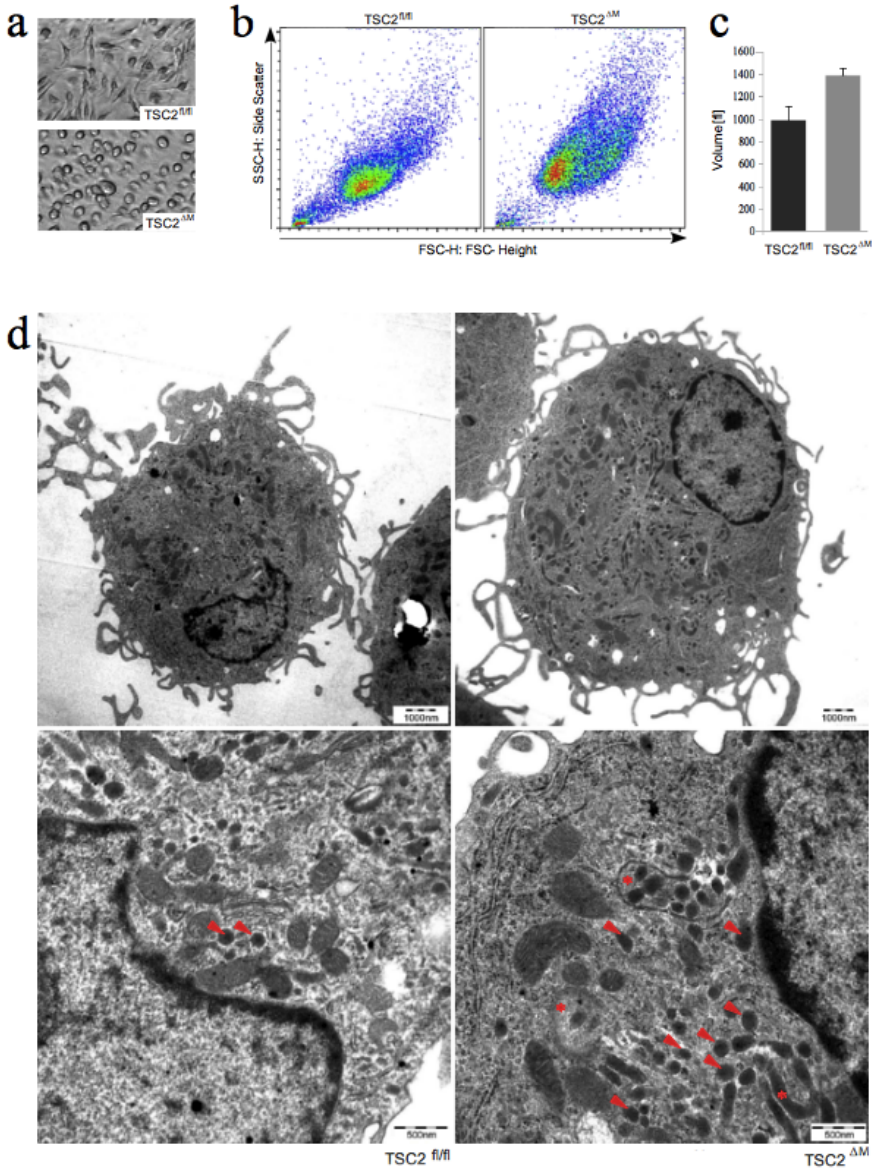

Figure 2: **Depletion of TSC2 alters cellular phenotype** BMDMs were seeded o/n in starvation medium A) on cell culture dishes and analyzed with light microscopy (Brightfield) and D) on glass slides and subjected to transmission electon microscopy. Red arrows indicate the mentioned electron dense organelles while red stars mark both growing phagophores and electron dense tubular structures (representative image of n=5; in different magnifications). In B) and C) BMDMs were analyzed by flow cytometry and Casy measurement after differenciation process (n=5 of 2 independent experiments, +SEM).

2.3 TSC2$^{\Delta M}$ BMDMs exhibit altered lysosomal and mitochondrial function

Electron dense organelles are usually referred to as lysosomes in the literature[76,77,78]. Thus BMDMs were stained for lysosomes with Lysotracker and subjected to flow cytometry (Fig.3a). Surprisingly, less fluorescence signal was measured in TSC2$^{\Delta M}$ BMDMs. Even though the precise action of this lysotrophic dye is unknown, it is usually referred as a reflection of lysosmal pH, consequently loss of TSC2 seemed to induce a malfunction in the acidification process. Additionally, the organelle marker LIMP2 was also reduced due the conditional knock-out of TSC2 when analyzed by immunofluorescence microscopy (Fig.3b). Western blot analysis confirmed this result, but the differences in normalized protein content were markedly less extensive (Fig.3c). This might suggest that LIMP2 is distributed more broadly in TSC2$^{\Delta M}$ BMDMs, thus producing a diffused picture in immunofluorescence.

Active mTORC1 is found on late endosomal/lysosomal surfaces and has also been shown to modulate TFEB, the so-called master-regulator of lysosomal biogenesis[61,62,105,69,70]. Western blotting showed a mobility shift of TFEB in TSC2$^{\Delta M}$ BMDMs, that upon rapamycin treatment shifted to the position that was observed in TSC2$^{fl/fl}$ BMDMs (Fig.3c). The faster running form of TFEB, as seen in TSC2$^{\Delta M}$ BMDMs, should predominately be found in the nucleus, as phosphatase treatment of lysates results in a lower running form of TFEB[105,69]. In line with these findings, we observed upregulation of established TFEB target genes, the h subunit of the v-ATPase and HEXA, while LIMP2 transcription was comparable in TSC2$^{\Delta M}$ and TSC2$^{fl/fl}$ BMDMs (Fig.3d). Interestingly, basal ERK phosphorylation was strongly reduced in TSC2$^{\Delta M}$ BMDMs, but was upregulated by rapamycin (Fig.3c). TFEB has also been shown to be a substrate of ERK[68], consequently modified mobility could also be due to lower or (upon rapamycin treatment) higher ERK activity.

Mitochondrial morphology was altered in knock-out BMDMs. Therefore, we accessed Mitotracker staining to investigate mitochondrial properties of BMDMs. Flow cytometry analysis showed an enhanced fluorescent signal in TSC2$^{\Delta M}$ BMDMs (Fig.3a). As mitochondrial metabolism of Mitotracker dye results in a green fluorescence, it can be used as a direct link to mitochondrial function. Additionally, a stronger signal for the β subunit of the mitochondrial F-ATPase was obtained by immunofluorescence staining of TSC2$^{\Delta M}$ BMDMs (Fig.3b). Therefore this data implicates enhanced mitochondrial activity and presence in TSC2$^{\Delta M}$ BMDMs.

Taken together, these results suggest a profound shift in cellular metabolism in the major anabolic and catabolic compartments of the cell. We found that TSC2 deplention compromised lysosomal pH and marker expression while a higher abundance of metabolic active mitochondria was observed. The later might either be a coping mechanism of macrophages to provide energy despite compromised lysosomes or a result of ineffective autophagic clearance. However, mTORC1 signaling is also known to promote mitochondrial biogenesis[58].

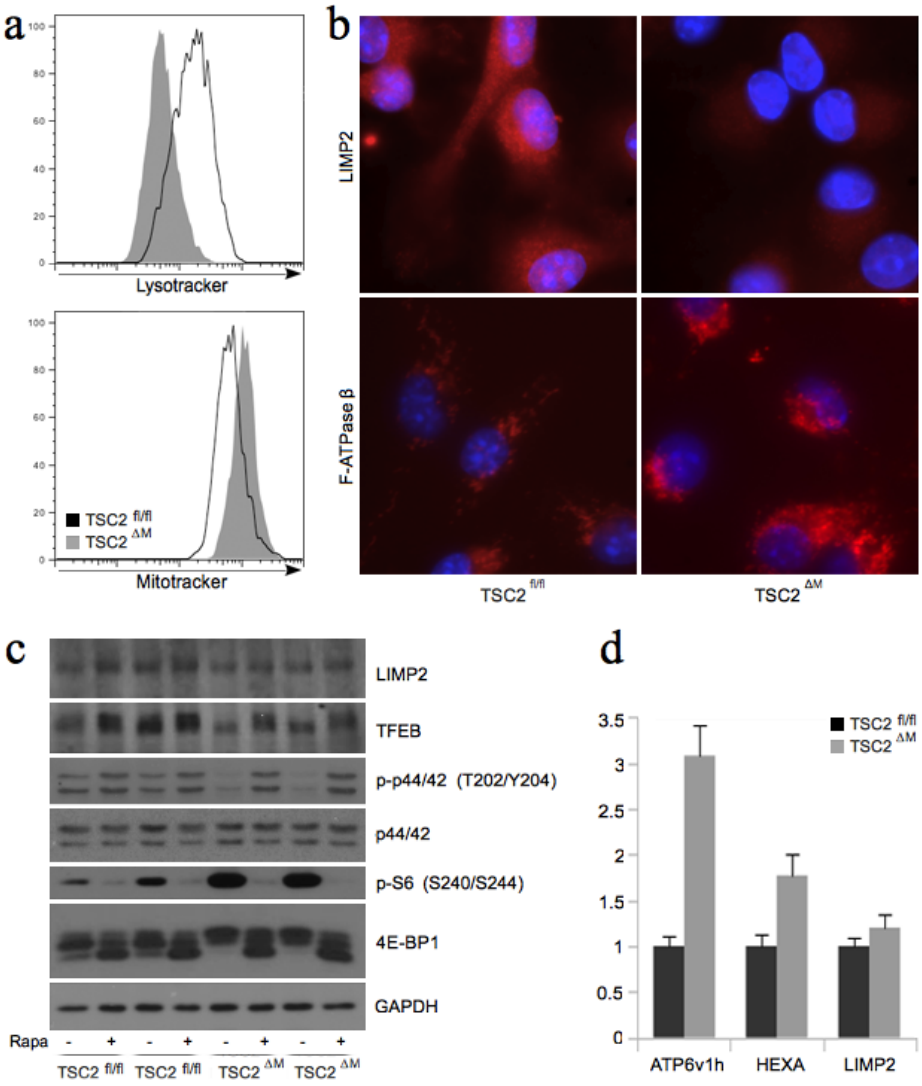

Figure 3: **TSC2$^{\Delta M}$ BMDMs show a shift in cellular metabolism** BMDMs were seeded o/n in starvation medium a) stained with Lysotracker and Mitotracker and analyzed by flow cytometry and b) stained for LIMP2 or the β subunit of the mitochondrial F-ATPase (red), couterstained with DAPI and analyzed with fluorescence-microscopy and c) were treated with rapamycin o/n or were left untreated. Cellular lysates were subjected to western blot and probed with the indicated antibodies and in d) were subjeted to qRT-PCR after 48h. Data represents mean expression levels normalized to TSC2$^{fl/fl}$ BMDMs=1, n=7 from 3 independent experiments, +SEM.

2.4 mTORC1 signaling alters endocytic and degradatory capacities of BMDMs

Next we wanted to investigate the functional result of TSC2 depletion and the role of mTORC1 signaling on lysosomal capacity of macrophages. As low-density lipoprotein (LDL) is exclusively degraded in the lysosome[99], fluorescent labeled LDL was used to monitor the flux of degradation in a time course dependent manner. Thus, BMDMs seeded o/n in lipoprotein-free media were fed Alexa488-LDL, which was removed by excessive washing after 30' (Fig.4a). Degradation and lysosomal acidification (Lysotracker) was monitored by fluorescence-microscopy. To determine the effects of mTORC1 signaling, BMDMs were treated with rapamycin o/n and further until the end of the time course. As a negative control the properties of the weak base chloroquine (CQ) were accessed. CQ raises the intracellular pH, thus impairs the degradation of LDL in the lysosome[106].

Remarkably, after 5h chase, $TSC2^{\Delta M}$ BMDMs contained nearly comparable amounts of labeled LDL as when they were treated with CQ, while only remnants of green staining were visible in $TSC2^{fl/fl}$ BMDMs (Fig.4a). As already shown by flow cytometry, $TSC2^{\Delta M}$ BMDMs showed decreased Lysotracker staining in comparison to floxed BMDMs. The observation that the uptake of labeled LDL was strongly elevated in $TSC2^{\Delta M}$ BMDMs was surprising, as under no condition we could see comparable green staining of $TSC2^{fl/fl}$ BMDMs. Importantly, $TSC2^{\Delta M}$ BMDMs treated with rapamycin showed a comparible kinetics as the non-treated floxed control. This indicates that all these processes — uptake, lysosomal pH and degradation capacity — are mTORC1 dependent.

To extend these results, a second assey was performed where the degradation of DQ-BSA was monitored by flow cytometry, whereas degradation of the BODIPY dye gives rise to fluorescent peptides. Surprisingly, although the amount of uptake was also highly elevated, $TSC2^{\Delta M}$ BMDMs degraded DQ-BSA faster than $TSC2^{fl/fl}$ BMDMs (Fig.4b). To be precise, $TSC2^{\Delta M}$ BMDMs dequenched double the amount of DQ-BSA, and degraded the resulting fluorescent peptides in the same time as $TSC2^{fl/fl}$ BMDMs. Although the cells were only pulsed for 15', the strongest fluorescence was observed at 0' chase, as seen before in THP-1 cells[107]. Thus dequenching was facilitated prior to or during uptake. Keeping in mind that BSA is a protein, continuous acidification along the endocytic route and the acquisition of diverse proteases of endocytic compartments, could be sufficient to for proteolysis of BSA.

Therefore, these results could be interpreted in different ways: Either lipoproteins belong to a handful of non-degradable targets due to constitutive mTORC1 signaling while the degratory capacity is similar for other substrates such as BSA. Or the bulk of BSA degradation is not facilitated in the lysosome, thus giving no insight if the lysosome might be able to degrade BSA. Collectively, these data shows that mTORC1 signaling promotes endocytic uptake of cargo and counteracts degradation of LDL while it promotes degradation of BSA.

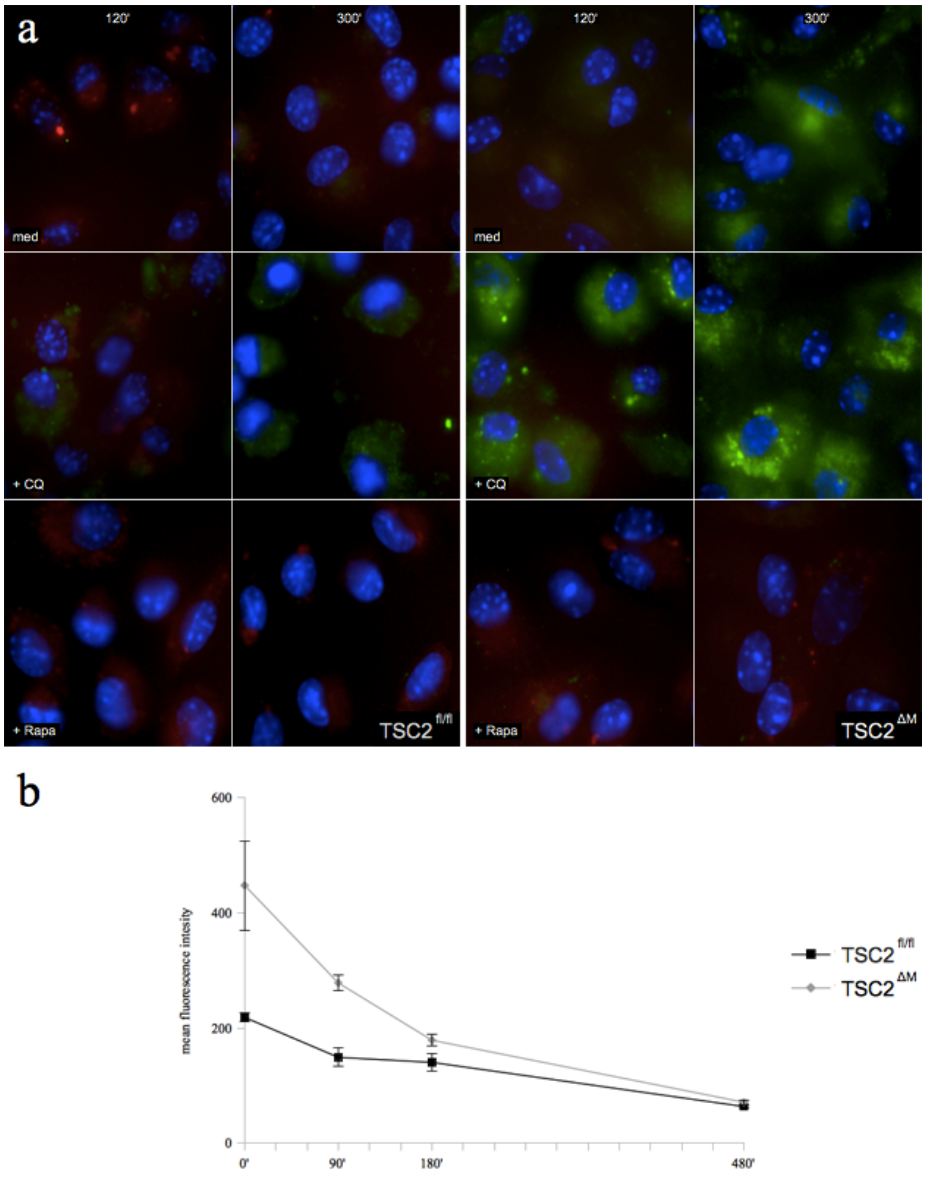

Figure 4: **TSC2$^{\Delta M}$ BMDMs show altered degradory capacity** BMDMs were seeded o/n a) in lipoproteinfree media and when indicated pre-treated with 100nM rapamycin o/n. 50μM CQ was added 30' prior pulsing the cells with 50μg/ml Alexa488-LDL. CQ and rapamycin were included until the end of the time course. BMDMs were fed Alexa488-LDL for 30', the stimulus was removed and degradation was chased for the indicated time points. Lysosomal acidification was assessed with Lysotracker and in b) BMDMs were pulsed with 10μg/ml DQ-BSA for 15', and dequenching/degradation was monitored by flow cytometry (n=4 of 2 independent experiments, +SEM).

2.5 Conditional knock-out of TSC2 pertubes tissue structure and function *in vivo*

To examine the effects of LysM dependent TSC2 depletion *in vivo*, various tissues were subjected to immunohistochemistry. In 10-12 weeks old mice clusters of hypertrophic cells were observed in internal organs, such as the spleen and the lung, in H&E stained sections, that were not found in control mice (Fig.5). The alveolar structure was greatly pertubed in $TSC2^{\Delta M}$ mice and in the spleen we observed a lack hemosiderin (yellow-brown patches), a sign of erythrophagocytosis. As removal of aged erythrocytes by the resident red pulp macrophages is one of the major functions of the spleen[26,108], this can be associated with a decline of tissue function. At 6 months of age the internal phenotype was even exuberated in $TSC2^{\Delta M}$ mice, accompanied by a strong swelling of paws and tails (Fig.6a&b). Interestingly, this was not due to oedema formation but represented a novel tissue, whereas the cells showed a similar phenotype to *in vitro* differentiated $TSC2^{\Delta M}$ BMDMs. We could confirm that these hypertrophic cells were macrophages, as they were not only positive for F4/80 but also for the macrophage marker MAC-2 (Fig.6c). MAC-2 positive histiocytes also showed a strong induction of p-S6, indicating constitutive active mTORC1 signaling (Fig.6a). It should be remarked that MAC-2 is not a frequently used macrophage marker, however it proofed to be the most reliable detectable marker, that always overlapped with p-S6.

Thus, conditional TSC2 depletion results in novel macrophage tissue formation in the skin and the appearance of hypertrophic macrophages in internal organs, disturbing tissue structure and function. Notable most of these cells were found in clusters near blood vessels, which could indicate either their dependence on nutrient supply or secondary infiltration.

2.6 mTORC1 inhibition reverses or prevents phenotype of $TSC2^{\Delta M}$ mice

We also set out to explore the role of mTORC1 signaling on the internal phenotype of $TSC2^{\Delta M}$ mice. Therefore 4 $TSC2^{\Delta M}$ littermates, 7 weeks of age, were treated orally with everolimus, while 2 received only the placebo. The treatment was performed daily for 4 weeks, whereafter the organs were subjected to immunohistochemistry. H&E stained sections showed that mTORC1 inhibition drastically reduced the presence of hypertrophic macrophages (Fig.7). In the lung the alveolar structure was restored and in the spleen there were again signs of erythrophagocytosis, although hemosiderin presence was lower than observed in $TSC2^{fl/fl}$ mice and found in clustered areas.

Therefore the presence of hypertrophic macrophages in various tissues is indeed mTORC1 dependent. Additionally removal of senescent erythrocytes in the spleen and a normal alveolar structure could be observed in everolimus treated $TSC2^{\Delta M}$ mice (Fig.7).

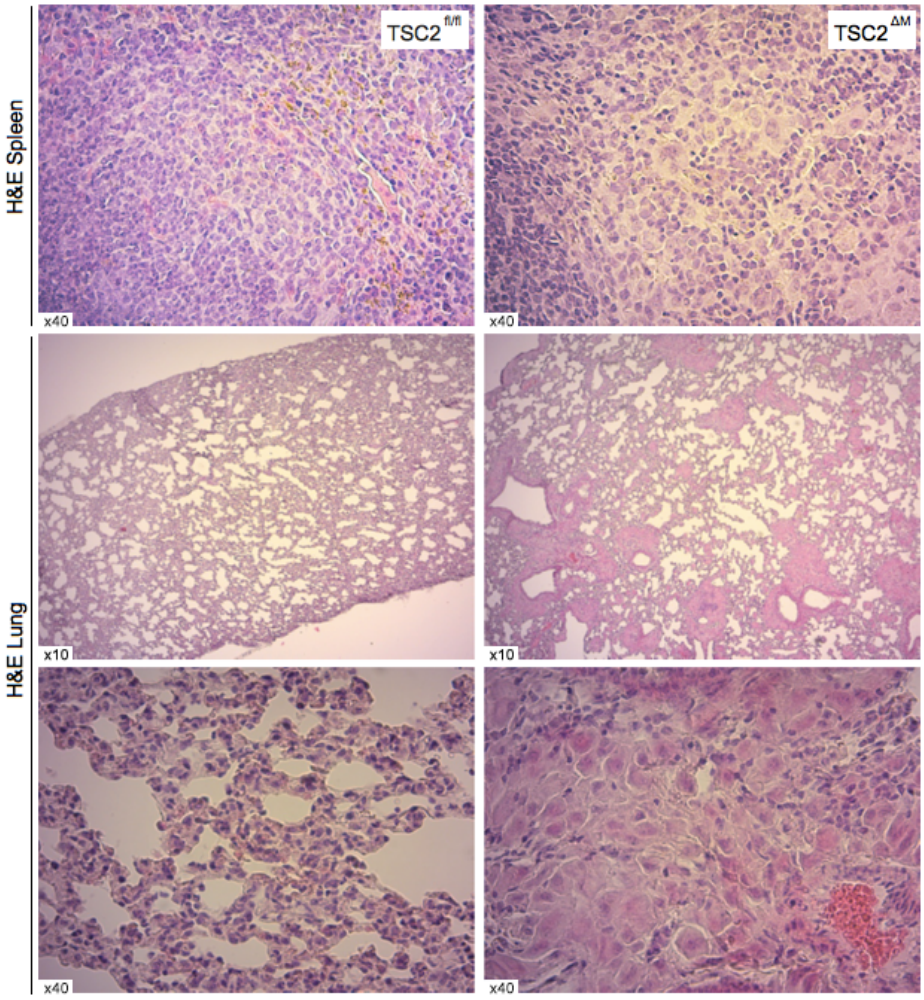

Figure 5: **LysM-dependent TSC2 depletion results in hypertrophic cell accumulation** Tissues of 10-12 weeks old mice were fixed, embedded in paraffin and sections were analyzed with H&E staining. Brown-yellowish patches in the splenic red pulp indicate hemosiderin, a sign of erythrophagocytosis.

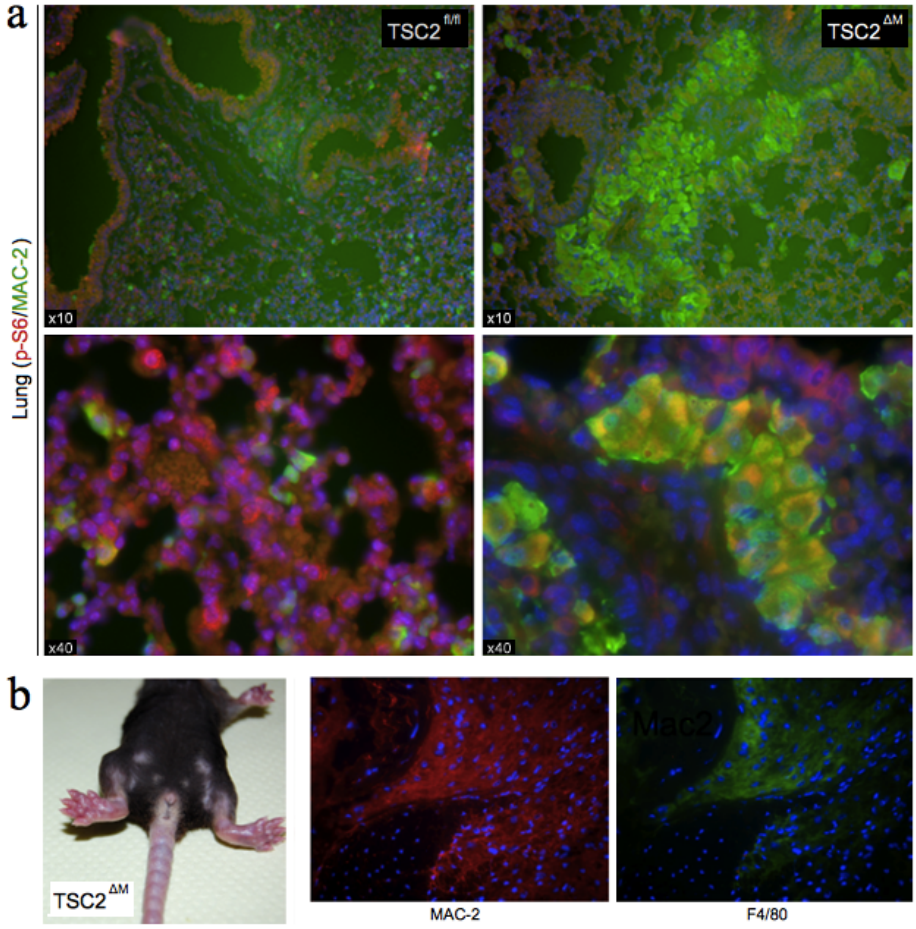

Figure 6: **LysM-dependent TSC2 depletion results in histiocyte accumulation** a) Lung and b) feet tissue of 6month old mice was fixed, embedded in paraffin and analyzed by immunofluorescence microscopy, whereas in a) p-S6 (red) MAC-2 (green) and in b) MAC-2 (red) F4/80 (green) secondary ABs were used, and counterstained withDAPI (blue). Additionally in b) a representative picture of $TSC2^{\Delta M}$ mice of 6 month is shown, whereas markedly swollen feet/legs and tail were observed.

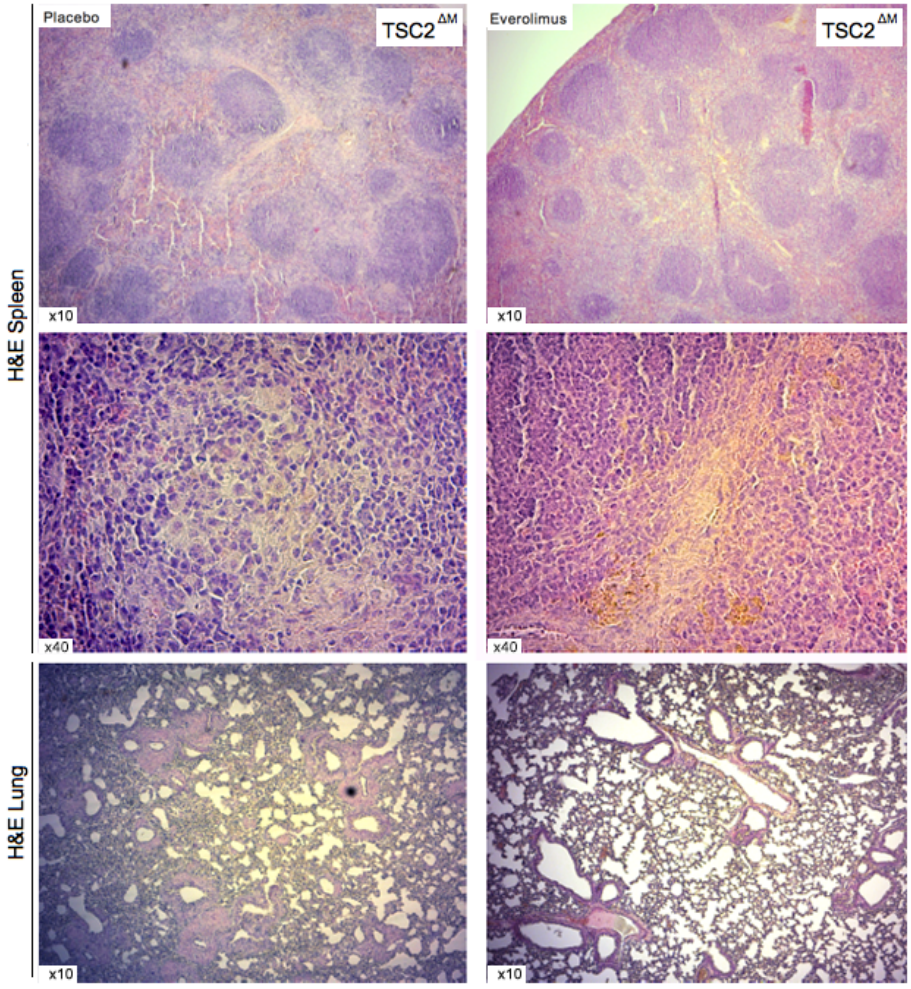

Figure 7: **Everolimus treatment reverses/prevents phenotype** 7 week old $TSC2^{\Delta M}$ mice were treated orally with everolimus (5mg/kg) for 4 weeks or received only the placebo. Subsequently tissues were fixed, embedded in paraffin and sections were analyzed by H&E staining.

3. Discussion

The mTORC1 signaling pathway has been shown to be decisive in a variety of immune cells, of both the adaptive and innate immune system[39,109,110,40]. In monocytes and macrophages, there is a growing amount of publications that focus on the role of mTOR in macrophage polarization, or the balance of pro- and anti-inflammatory cytokine secretion[111,112,113,49]. In contrast, this study shows that the TSC2-mTORC1 pathway modulates lysosomal capacity of murine macrophages.

3.1 Altered endo-lysosomal kinetics and mitochondria in TSC2$^{\Delta M}$ BMDMs

LysM-dependent TSC2 depletion resulted not only in constitutive mTORC1 signaling but also grossly changed the phenotype of BMDMs. TSC2$^{\Delta M}$ cells appeared highly granular, big and round *in vitro*. Although mTORC1 is considered to be a master-regulator of growth[51,29,27], the granularity pointed to a more substantial change of cellular morphology and functionality. Electron microscopy showed a multitude of electron dense organelles in TSC2$^{\Delta M}$ BMDMs, which we considered to be lysosomes according to their ultrastructure. Markedly, they were also observed in growing autophagic structures, although mTORC1 signaling is usually accepted to exert an inhibitory function on autophagy[29,27,114]. This strongly hints to a malfunction of these electron dense organelles and it has been shown only recently that also damaged lysosomes are subjected to autophagy[115].

There are further experiment necessary to explain this phenomena, however autophagy may occur also independent of mTOR signaling[114]. Additionally, no closed autophagic vacuole was seen in any of the examined cells. Therefore autophagic progression seemed to be inhibited in TSC2$^{\Delta M}$ BMDMs. Thus, although autophagy is obviously initiated to sequester hypothetical damaged or malfunctioning organelles (despite constitutive mTORC1 signaling), phagophore progression seems to be counteracted by TSC2 depletion.

Additionally, structures of tubular shape with similar electron dense appearance seemed to be "growing" in the junxanuclear region of TSC2$^{\Delta M}$ BMDMs, that could not be found in TSC2$^{fl/fl}$ macrophages. This resembled a maturation

process, probably to replenish defective organelles.

The morphology of those electron dense organelles pointed to lysosomes and there are several links of mTORC1 signaling to the lysosome. First, mTORC1 is targeted to the late endosomal/lysosomal surface, by the Rag-GTPases, where the active signaling process is thought to take place[61,63]. At the lysosome the pentameric Ragulator complex, while interacting with the v-ATPase, functions as a GEF for the Rags, thus promoting the amino acid dependent shuttling of mTORC1 to the lysosome[62,64]. Additionally proton pumping of the v-ATPase appears to be required for amino acid sensing of mTORC1, which curiously seems to be independent of lysosomal acidification[63].

Secondly, mTORC1 signaling regulates TFEB, which upon nuclear translocation, upregulates an entire repertoire of lysosomal and autophagic genes[67,68]. However, there are controversial results as to how mTORC1 is influencing TFEB. While one group showed that mTORC1 promotes nuclear translocation of TFEB[105], other studies propose that mTORC1 signaling actually counteracts the nuclear accumulation of TFEB[69,70]. In the literature there are more indications that point to the later view, however, the majority of the data is obtained by overexpression of TFEB, which might disturb physiological conditions. There are also indications that TFEB can[105,71], or can not be modulated with rapamycin, but only with ATP-competitive inhibitors of mTOR[69,70]. Regardless, TFEB has been shown to be a mTORC1 target multiple times, and maybe the identification of its phosphatase will elucidate its regulation in more detail.

When we investigated the abundance of lysosomes in BMDMs, the lysosomal marker LIMP2 as well as Lysotracker staining was reduced in $TSC2^{\Delta M}$ cells. This indicated that there are actually less, or at least less functional lysosomes present. We observed no decrease in LIMP2 mRNA levels in comparison to $TSC2^{fl/fl}$ BMDMs and normalized protein comparison by western blot analysis showed only a slight reduction of LIMP2 in $TSC2^{\Delta M}$ BMDMs. This stands in contrast to data obtained by immunofluorescence, but in the aspect of the multiply "newly" formed organelles, availible LIMP2 might be scattered, thus giving the impression of the presence of less lysosomes. Additionally, changes in LIMP2 translation and aberrant endo-lysosomal trafficking or fusion, should be considered as a cause for the reduction of LIMP2 observed in immunofluorescence.

The altered mobility shift of TFEB observed in $TSC2^{\Delta M}$ BMDMs was indeed reversible by o/n rapamycin treatment. Although there are conflicting results regarding the nature of mTORC1-dependent regulation of TFEB, they are in agreement that hyper-phosphorylated TFEB is retained in the cytoplasm[105,69,71,70]. Phosphatase treatment of lysates results in a lower running form of TFEB[105,69], hence, TFEB in $TSC2^{\Delta M}$ BMDMs should predominantly be found in the nucleus. In agreement with this, we also observed an upregulation of TFEB target genes HEXA and the h subunit of the v-ATPase[67].

Although $TSC2^{\Delta M}$ BMDMs were seemingly perturbed in their catabolism, they exhibited increased mitochondrial abundance and function. This was accessed by immunofluorescence of the β subunit of the mitochondrial F-ATPase

and measuring Mitotracker by flow cytometry. When metabolized, Mitotracker dye resulted in green fluorescence, which was elevated in TSC2$^{\Delta M}$ BMDMs, as was F-ATPase-β staining. Although this is in line with the literature, in combination with lysosomal malfunction, this could be a coping mechanism to support cell growth/viability. The rational for examining mitochondria function, however, was their irregular shape observed in electron micrographs. Thus it could also imply that mitochondrial turnover is limited due to TSC2 depending lysosomal dysfunction.

To determine if this complex cellular phenotype is indeed altering the degradory capacity of macrophages, we challenging BMDMs to degrade either LDL or DQ-BSA, which surprisingly lead to opposite outcomes. LDL removal was clearly hampered in TSC2$^{\Delta M}$ BMDMs, while a higher amount of DQ-BSA was processed in a comparable time frame as in TSC2$^{fl/fl}$ BMDMs. We accessed LDL, as its degradation is completely dependent on the lysosome [99]. BMDMs deprived of lipoproteins o/n were pulsed with Alexa488 labeled LDL for 30' and thereafter chased in fresh media. At various time points the cells were co-stained with Lysotracker, to monitor lysosomal acidification during this process. However, even after 5h chase, TSC2$^{\Delta M}$ BMDMs seemed to be unable to degrade LDL, as there fluorescent intensity was nearly comparable as when treated with CQ (which raises the intracellular pH). Rapamycin treatment lead to a comparable LDL flux in TSC2$^{\Delta M}$ BMDMs as observed in TSC2$^{fl/fl}$ BMDMs, as well as Lysotracker staining, which provides evidence that these processes are mTORC1 dependent. Additionally, we also saw that the uptake capacity of LDL is strongly elevated in TSC2$^{\Delta M}$ BMDMs. The most straightforward explanation could have been that this is not mTORC1 but solely TSC2 mediated, as TSC2 has been shown to act as a GAP toward RAB5 and this small GTPase is playing a key role in endocytosis and early endosome dynamics [116,41]. This however can be ruled out, as also this process was reversible upon rapamycin treatment. Of note, RAB5 activity is modulated by PI3K, thus early endosome kinetics might be specifically modulated by the negative feedback loop to IRS1, induced due to mTORC1 hyperactivation [41]. Regardless, this data implicates a fundamental role of mTORC1 in endocytic uptake, lysosomal pH and degradation capacity in macrophages.

To our surprise we found that although endocytic uptake was comparable elevated towards DQ-BSA in TSC2$^{\Delta M}$ BMDMs, they were able to degrade DQ-BSA faster than TSC2$^{fl/fl}$ BMDMs. The strongest fluorescence was observed at 0', which was surprising, as the cells had been only pulsed for 15'. It should be remarked that in this experimental setup, a reverse outcome was expected — not a decrease in fluorescence but an increase. As, according to the manufacturer DQ-BSA proteolysis results in dequenching of its conjugated dye BODIPY, and the resulting peptides are strongly fluorescent. However although the cells were only pulsed for 15', the strongest fluorescence was observed at 0' chase. Importantly this has been observed before in THP-1 cells [107]. Thus dequenching is already facilitated within this 15' either due to secreted proteases or those that are already present in the EE. That secreted proteases are the key here might

be surprising: the media was prepared in advance, DQ-BSA added prior cells were washed, thereafter the pulsing media was immediately added to the cells. It has been reported that macrophages are capable to renew at least half of their plasma-membrane (up to 148%) in 30'[117]. Thus endosomal compartments are secreted, which could mean that 15' are enough to secrete an sufficient amount of proteases. It is questionable, however, if the degradation of the resulting peptides is limited to the lysosome,as there are other ways to break down proteins, such as the proteasome. Also, endosomes on route to the lysosome constantly aquire a lower pH and proteases[76,77,82], which might be sufficient to break down BSA in a pre-lysosomal compartment.

In summary, degradation kinetics of Alexa488-LDL were clearly perturbed in TSC2$^{\Delta M}$ BMDMs, but rescued upon rapamycin treatment. Thus constitutive mTORC1 signaling might either compromise lysosomal degradation of lipoproteins and similar targets in particular, while promoting the flux of other substances such as DQ-BSA, or the later is not specifically dependent the lysosome for degradation. The data draws an interesting picture that raises the question about the maturation capability of endosomes and endo-lysosomal fusion due to TSC2 depletion. It, however, clearly indicates that mTORC1 hyperactivation is counteracting lysosomal degradation of at least lipoproteins and maybe similar targets. Selectively exclusion of specific substrate degradation (depending on the genetic defect) is a hallmark of LSDs, although further accumulation of these substances globally disturbes lysosomal capacity[84,91,92]. Therefor differential degradation kinetics actually highlight the comparable aspects of TSC2$^{\Delta M}$ macrophages and LSDs.

3.2 Mechanistic implications of mTORC1 in v-ATPase and TFEB regulation

How does constitutive mTORC1 signaling perturb lysosomal function? It is tempting to hypothesize that cellular positioning of active mTORC1 on the lysosome has a direct effect. However, both amino acid stimulation as well as mTORC1 inhibition induce lysosomal clustering of mTORC1[118,70,119]. Since activation and inhibition induce mTORC1 translocation to the lysosome, it should be the action of the signaling complex that directly mediates lysosomal capacity.

The reduction of Lysotracker staining in TSC2$^{\Delta M}$ BMDMs pointed to a defect in lysosomal acidification. Importantly, this could be rescued by rapamycin treatment, thus was mTORC1 mediated. The v-ATPase not only acidifies cellular compartments, but also serves as an anchor for Ragulator and active mTORC1 to late endo/lysosomal structures[83,82,81,62,64]. Additionally, this multimeric complex undergoes subunit isotypes exchange upon endosomal transition, and the V1 domain can dissociate from the membrane anchored V0 domain[81]. Subunit exchanges are crucial for normal cellular function, also of other compartments of the cell beside the endo-lysosomal pathway. For example,

a loss-of-function mutation of the human a2 isotype causes for aberrant protein glycosylation in the golgi[120]. Interestingly, there are indications that the dissociation/assembly process is at least under certain conditions regulated by PI3K or the PI3K-mTOR pathway. Bone resorption of osteoclasts is disrupted upon PI3K inhibition, as it prevents the re-location of the a3 subunit containing V1 domain to the plasma membrane[121,122]. This is apparently facilitated due to an interaction of PI3K with F-actin, which promotes ruffled border formation[122]. It was proposed that the glycolytic enzyme aldolase, acts as a glucose-sensor, while interacting with subunits of the v-ATPase[123]. Upon glucose stimulation it mediates reassembly of the v-ATPase, to promote acidification of intracellular compartments, which can also be mimicked by a constitutive active p110α subunit and reversed by PI3K inhibition[123,124]. However, there are no follow-up publications, if this process is also mTORC1 dependent, which is not only activated by glucose but also promotes glucose uptake and glycolysis[56,59].

As in all the experiments, long term (o/n *in vitro*, or 4 weeks *in vivo*) rapamycin treatment was performed, indirect effects might rescue lysosomal function. Such as protein expression induced by TFEB, the master regulator of lysosomal and autophagic genes. Curiously TFEB appeared to be less phosphorylated in TSC2$^{\Delta M}$ BMDMs in the steady-state, which is contradictory to the bulk of mTORC1-TFEB publications. Thus TFEB should be targeted to the nucleus, which we indirectly confirmed by qPCR, as we observed upregulated transcription of TFEB targets, the H subunit of the v-ATPase as well as HEXA. Additionally, the tubular structures in electron microscopy pictures also indicated an active maturation process. The data draws a very complex picture, as lysosomal genes are higher expressed upon TSC2 depletion, a process that is probably TFEB dependent, but physiological conditions are not reached during constitutive mTORC1 signaling. Enhanced TFEB transcriptional activity and continous lysosomal maturation, probably to counteract storage, were also observed in some storage diseases, although in others its activation has been suggested as a therapeutic target[84,92].

Interestingly, Yu *et al.* showed that lysosomal reformation from autolysosomes also seems to be an mTORC1 dependent process. Accordingly, degradation of autolysosomal substrates induces mTORC1 reactivation, which thereafter promotes pinching of lysosomes in a clathrin dependent manner[125,126] Thus, constantly activated mTORC1 might mimic a post-catabolic state to counteract cell-mass decrease in a seemingly nutrient rich environment. It is notable that newly formed lysosomes still have to recover the physiological acidic pH of lysosomes[125].

The presence of TFEB at the lysosome is apparently also mediated by the Rag GTPases in an amino acid dependent manner[127]. However, we neither know about the available amino acid pool within TSC2$^{\Delta M}$ BMDMs, nor the preferential interaction partner of GTP loaded Rags, as mTORC1 could be favoured. Thus the process of mTORC1 dependent phosphorylation of TFEB (to promote its retention in the cytoplasm), might be abrogated upon sequestering cellular locations of those two key players. Additionally, it should be mentioned that in addition to the Rag GTPases, a second signaling event is mediating nutrient

availability to mTORC1. Amino acid- or glucose-induced phosphatic acid production by phospholipase D (PLD1) is mediated by vacuolar protein sorting 34 homologue (Vps34), and phosphatic acid is known to promote Rheb activity[128].

Interestingly, the modulation of TFEB was first ascribed to the activity of ERK. Accordingly, MAPK-inhibitors induced TFEB nuclear translocation, as did ERK knock-down, while opposite effects were obtained by EGF treatment or constitutive active MEK[68]. And in a new report, ERK phosphorylation and activation has been shown to be spaciotemporal linked to autophagosomal surfaces[129]. Autophagic progression seemed to be affected in $TSC2^{\Delta M}$ BMDMs and we also found that basal ERK phosphorylation was abolished in $TSC2^{\Delta M}$ BMDMs, which was rescued upon rapamycin treatment. Thus, nuclear translocation of TFEB in $TSC2^{\Delta M}$ BMDMs might be an ERK dependent phenomena. The reliance of MEK-ERK function on autophagosomal structures could explain the loss of ERK phosphorylation, due to defective autophagosomal progression/closure. Phagophore initiation despite mTORC1 signaling, might be a secondary effect due to constitutive mTORC1 signaling. In growth factor absence, the p110β subunit of PI3K has been shown to dissociate from its receptor to activate the lipid kinase Vps34 via RAB5 to promote phagophore initiation[130,131]. And in our system the negative feedback loop via IRS1 is activated, thus counteracting PI3K activation and possibly promotes autophagy initiation.

But how fundamental is the role of TFEB in lysosomal function? Zhou *et al.* actually showed that both starvation and catalytic inhibition of mTORC1 potently activates lysosomal acidification. And while the transcriptional efforts of TFEB are required, the actual activation of the lysosome (or lysosomal acidification) is dependent on auto-lysosomal fusion[119]. Of note, the machinery for phagocytosis and endocytosis is similar for autophagy, although these pathways function in parallel[22].

3.3 mTORC1 signaling in macrophages and tissue homeostasis

The *in vivo* phenotype observed in $TSC2^{\Delta M}$ mice hinted towards a lysosomal disorder. Accumulation of hypertrophic cells in various tissues could be already observed in 10-12 week old $TSC2^{\Delta M}$ mice, a feature that was intensified at 6 month of age. No comparable phenotype could be seen in any of the examined $TSC2^{fl/fl}$ tissues. A strong p-S6 signal was always correlating with the macrophage-associated marker MAC-2, indicating a strong activation mTORC1. These cells were mostly found in clusters, in close proximity to blood vessels and their presence was clearly altering tissue function to the worse. Especially in the lung we could see a clear disturbance of the alveoli, which can be associated with a reduction of available area for gas-exchange. Additionally, alveolar macrophages sitting within the alveolar space could hardly be found. Thus, either alveolar macrophages migrate towards the hypertrophic cells to

remove them, but are unable to do so, or they are themselves affected by the knock-out. Of note, alveolar macrophages expess high levels of MAC-2[9] and belong to the non-bone marrow derived tissue macrophages that have been shown to replenish themselves[6,15,8]. GM-CSF-dependent alveolar macrophages are also crucial for lung homeostasis[15 132]. Moreover, ineffective clearance of surfactant by alveolar macrophages, induces pulmonary alveolar proteinosis (PAP). Surfactant is a mixture of proteins and lipids, that prevent alveoli from collapsing, whereas surfactant proteins are central in pulmonary host defense. Surfactant is constantly secreted by alveaolar type II cells and scavenged by alveolar macrophages. Thereby this protective coat is gradually renewed while being sampled for microbes. This system is disturbed in PAP and lipid-laden alveolar macrophages accumulate in the lung[132]. The macrophage phenotype observed in PAP is similar to TSC2 depleted macrophages and this notion is also supported by their disturbed LDL degradation kinetics. In the spleen we observed a functional alteration of a tissue-resident population. Red pulp macrophages are responsible for the bulk removal of aged erythrocytes and play a prominent role in the recycling of heme-derived iron[26,108]. This process is visible as hemosiderin deposits — a yellowish brown granular pigment formed by breakdown of hemoglobin. However, we could not find an indication of this process in young $TSC2^{\Delta M}$ mice, as hemosiderin was completely absent in H&E stained sections.

To determine the role of mTORC1 in the accumulation of macrophages in tissues, we treated $TSC2^{\Delta M}$ littermates, 7 weeks of age, orally with everolimus. Meanwhile, others received the placebo, which as the rapaloge, was administered once daily for 4 weeks. Importantly, everolimus-treated $TSC2^{\Delta M}$ mice showed markedly reduced hypertrophic macrophages in internal organs. H&E stained tissues also indicated that erythrocyte turn-over was elevated in treated mice. We could again see hemosiderin staining in the spleen, although in more compact structures and overall less compared to untreated $TSC2^{fl/fl}$ spleen. This might reflect the areas that were more accessible to circulating drug supply. Decrease in overall hemosiderin deposits might be due to long-term treatment of mice, probably bulk removal of aged erythrocytes occurred earlier during the treatment. As in the spleen, the structure of the lung was restored, or the accumulation of hypertrophic macrophages was prevented upon everolimus treatment. Thus we can conclude that clustering macrophages in tissues of mice is an mTORC1 dependent phenomen.

There are prominent LSDs that affect primarily macrophages, such as Gaucher type I and Niemann-Pick disease, where an aberrant accumulation of hypertrophic macrophages in tissues is observed[133]. Clearly the dependence of phagocytes on their "digestive tract" makes them highly susceptible to LSDs. Although the mTOR pathway is often referred to a signaling pathway that promotes proliferation and cell survival, the exact mechanism of macrophage accumulation in $TSC2^{\Delta M}$ mice remains elusive, which is also true for macrophage expansion in LSDs. An important puzzle-piece might be a recent finding by Hsu *et al.*, showing that lysosomal malfunction (induced by the deficiency of a lysosomal nucleoside exporter) lead to macrophage expansion *in vivo*[134]. The main mechanism seemed to be constitutive signaling of colony stimulating factor

receptor 1 (CSFR1), which upon activation promotes both macrophage differentiation and proliferation[9,10]. Growth factor binding usually induces CSFR1 endocytosis and degradation, however perturbed lysosomal function lead to stabilization of the receptor and therefore aberrant signaling and macrophage expansion[134]. This concept of macrophage expansion could at least partially explain macrophage accumulation in TSC2$^{\Delta M}$ mice. However, decreased apoptosis or enhanced infiltration/migration of monocytes/macrophage have to be also taken into consideration.

3.4 Conclusion and Outlook

Collectively this thesis shows that LysM dependent TSC2 depletion results in a metabolic shift in macrophages, whereas enhanced mitochondrial metablolism is mirrored by compromised lysosomal function. Phenotype manifestation observed *in vitro* as well as *in vivo* are comparable to features observed in LSDs. Implying that a re-evaluation of mTORC1 activity for certain lysosomal disorders might suggest alternative treatments, especially in the aspect of highly specific available drugs to target the mTOR-pathway.

Additionally these observations raise several interesting questions regarding mTORC1 signaling in in the course of an inflammatory process, as mTORC1 is known to be activated in macrophages upon TLR engagement. Is TLR engagement modulating lysosomal function in macrophages *in vivo*? One might argue that it would be counterproductive to decrease lysosomal capacity during an infection, on the other hand a less acidic pH seems to promote antigen presentation to adaptive immune cells[135,136], thus is actually promoting an adaptive immune response. Are lysosomal alterations required to carry out certain effector functions and when is it necessary or even harmful to the body? Answering this questions will probably provide alternative medical strategies in progressive myeoloid diseases and enhance our understanding of macrophage biology in various aspects of inflammation and tissue homeostasis.

4. Materials & methods

4.1 Cell culture

4.1.1 Medium and solutions

BMDM differentiation media

⋆ DMEM 4.5g glucose/l (Gibco)
⋆ 10% low endotoxin FBS (PAA)
⋆ 2mM L-glutamine (PAA)
⋆ 60mg/l penicillin(Sigma)
⋆ 100mg/l streptomycin (Sigma)
⋆ 50nM β-mercaptoethanol (Gibco)
⋆ 10-20% L929 conditioned Media)

BMDM starvation media

⋆ DMEM 4.5g glucose/l (Gibco)
⋆ 2% low endotoxin FBS (PAA)
⋆ 2mM L-glutamine (PAA)
⋆ 60mg/l penicillin(Sigma)
⋆ 100mg/l streptomycin (Sigma)
⋆ 50nM β-mercaptoethanol (Gibco)

L929 expansion media

⋆ DMEM 4.5g glucose/l (Gibco)
⋆ 10% FBS (PAA)
⋆ 2mM L-glutamine (PAA)

L929 starvation media

⋆ DMEM 4.5g glucose/l (Gibco)
⋆ 2mM L-glutamine (PAA)

Liporotein-free media

⋆ DMEM 4.5g glucose/l (Gibco)
⋆ 10% lipoprotein-free FBS (kindly provided by Herbert Stangl)
⋆ 2mM L-glutamine (PAA)
⋆ 60mg/l penicillin(Sigma)
⋆ 100mg/l streptomycin (Sigma)
⋆ 50nM β-mercaptoethanol (Gibco)

10xRBC (red blood cell) lysis buffer pH7.3

⋆ 82,6g Ammonium Chloride
⋆ 10g Potassium Bicarbonat
⋆ 0,37g EDTA
⋆ HCl to adjust pH
⋆ fill up to 1l with dH_2O
⋆ sterile filter

4.1.2 Cell culture conditions

All procedures were performed under sterile conditions (MSc Advantage biological safety cabinet, Thermo Scientific, Waltham, MA, USA) and cells were kept at 37°C, 5%CO_2 and 80% humidity (Heraeus BBD 6220, Thermo Scientific).

4.1.3 BM isolation and BMDM differentiation

Femurs and tibias were cleansed of excess tissue, sterilized in 70% EtOH and placed into DMEM. BM was flushed out, using a syringe and a 0.9mm needle and was either frozen, or seeded for differentiation immediately. For freezing BM was treated for 3min with sterile filtered 1xRBC lysis buffer on ice and 2% FBS supplemented PBS was used to stop lysis. Thereafter BM was frozen in 90%FBS and 10%DMSO and kept in liquid nitrogen tank until further usage. Whole BM (2xfemur; 2xtibia) was seeded on five 10cm petri-dishes in 12ml differentiation media. On day 4 floating cells were removed by 1xPBS washing, as unlike other cells macrophages stick on the non-treated plastic dish. Adherent cells were dislocated by gentle scraping with a rubber policeman (CytoOne) and splitted 1:2. On day 7 cells were washed and macrophages were harvested as above, counted and seeded for experiments in indicated media.

L929 conditioned media

L929 cells, which in culture produce M-CSF, were seeded on 15cm cell culture dishes in expansion medium. For 1L conditioned media, approximately 40 plates were needed. When 60% confluent, cells were washed twice with 1x PBS and 30ml L929 starvation media was added. After 10-11 days supernatant was harvested, sterile filtered and stored at -80°C. Each batch was tested for its efficiency to generate BMDMs in different concentrations (10-20%) before further usage.

4.2 Casy measurement

Cell volume determination was performed using the CASY Cell Counter, Model TTC (Schaerfe System). Cell were diluted in 10 ml of CASYton isotonic dilution buffer and 0.4 ml of total volume were then measured in triplets.

4.3 Flow cytometry

For flow cytometry 3-4x10^5 cells/well were seeded in 12-well plates. For DQ-BSA degradation, cells were pulsed for 15min with 10μg/ml DQ-BSA (Molecular Probes), washed 3x with PBS and chased in fresh media until they were subjected to flow cytometry. For accession of lysosomal acidification and mitochondrial metabolism BMDM were treated for 30min with 60nM Lysotracker or Mitotracker (both Molecular Probes) in starvation Media in the incubator.

Cells were placed on ice, were washed twice with PBS, dislocated by gentle scraping in FACS buffer (2%BSA, 2mM EDTA/PBS) and data obtained with BD FACSCalibur flow cytometer (BD) was analyzed using FlowJo (TreeStar).

4.4 Immunofluorescence

BMDM (4-8x10^5 cells/well) were seeded in 4- or 8-well chamberslides in starvation media o/n. Cells were washed the next day and fixed with 4% PFA for 10min on RT. All following steps were performed at RT unless otherwise indicated. After 3x washing with PBS, excess PFA was quenched with 100nM Glycine/PBS for 15min. Thereafter cells were washed for 30min with PBS and permeabilized with 0.5% TritonX/PBS for 7min. Slides were washed trice with PBS and than incubated with PBS for 30min. For blocking, slides were incubated with 1% BSA/PBS for 60min whereafter the chambers were removed and slides were rinsed well with PBS. After o/n incubation at 4°C with the primary antibody in PBS, slides were rinsed with PBS and incubated 3x20min in PBS. Secondary antibody was incubated for 60min, whereafter slides were rinsed and incubated 2x20min in PBS. Nuclei were stained with DAPI (1:2000; Roth) for 20min at RT. Slides were rinsed with PBS, mounted with VECTASHIELD (Vector Laboratories) and sealed with nail polish. Cells were analyzed using a Axiophot fluorescent microscope (Zeiss).

Specificity	**Label**	**Species**	**Dilution**	**Company**	**Catalog no**
LIMP2	none	rabbit	1:100	NovusBiol	NB400-129
F-ATPase β	none	rabbit	1:250	Abcam	MS503
Rabbit IgG	Alexa 546	goat	1:10000	Invitrogen	A1004

4.4.1 LDL degradation assay

4x10^5 cells were seeded in 8-well chamberslides (Sarstedt) in liporotein-free media. When indicated cells were pre-treated with 100nM rapamycin (Calbiochem) after adherence, which was included until the end of the time course. The next day they were pulsed with 50μg/ml LDL-Alexa488 for 30min, then cells were washed trice with PBS and degradation was chased in lipoprotein-free media. For lysosomal inhibition cells were pre-treated for 30min with 50μM/ml CQ (Sigma) before LDL-pulse, which was also included until the end of the time course. Lysotracker (Molecular Probes) was included at 60nM for 30min prior fixing of cells. Therefore chambeslides were placed on ice, washed 3x with PBS and fixed with 4% PFA for 30min at 4°C. PFA was removed by washing trice as above, chambers were removed and cells were counter-stained with DAPI (1:2000) for 20min at RT. Slides were rinsed with PBS and mounted with VECTASHIELD (Vector Laboratories) and sealed with nail polish.

Preparation of LDL-Alexa488

Human LDL (kindly provided by Herbert Stangl) was dissolved well in PBS (1mg/440μl) and mixed with 50μl 1M $NaHCO_3$. 100μg Alexa488 dye (Invitro-

gen) was added and icubated at RT for 1h on the belly dancer. A Sephadex column (Sephadex G-25; 0.7g in 7 ml PBS) was prepared to separate labeled LDL from free labeling dye. As labeling dye was added in excess, the volume of labeled LDL was used to estimate concentration of labeled LDL (usually c=1.3 - 1.5mg/ml), which was stored light protected at 4°C.

4.5 Western blot

4.5.1 Buffers and solutions

Buffer A
- ⋆ 20mM Hepes pH 7.9
- ⋆ 0.4M NaCl
- ⋆ 25% (v/v) Glycerin
- ⋆ 1mM EDTA
- ⋆ 0.5mM Na_3VO_4
- ⋆ 0.5mM DTT

PIM
- ⋆ 200μg/ml Leupeptin
- ⋆ 200μg/ml Aprotinin
- ⋆ 30μg/ml Benzomidinchloride
- ⋆ 1mg/ml Trypsininhibitor
- ⋆ 0.5mM Na_3VO_4
- ⋆ 0.5mM DTT

Lysis buffer (1ml)
- ⋆ 860μl Buffer A
- ⋆ 20μl PIM
- ⋆ 10μl 100mM PMSF
- ⋆ 100μl 10x Prot. inh. (Roche)
- ⋆ 10μl TritonX 100

10xTBS
- ⋆ 1.5M NaCl
- ⋆ 0.5M Tris pH7.4

4x SDS loading dye
- ⋆ 200mM Tris pH6.8
- ⋆ 1M DTT
- ⋆ 8% (w/v) SDS
- ⋆ 0.4% (w/v) Bromphenolblue
- ⋆ 40% (v/v) Glycerol

10xRunning buffer
- ⋆ 60.6g Tris
- ⋆ 292g Glycine
- ⋆ 100ml 20% (w/v) SDS
- ⋆ dH_2O up to 2l

Harlow buffer
- ⋆ 29g Tris
- ⋆ 145g Glycine
- ⋆ 25ml 20% (w/v) SDS
- ⋆ 1l MeOH
- ⋆ dH_2O up to 5l

1xTBST
- ⋆ 100ml 10xTBS
- ⋆ 1ml TritonX 100
- ⋆ dH_2O up to 1l

4.5.2 Whole cell lysate preparation

For western blot 2- $3x10^6$ cells were seeded in 6-well plates in starvation media and after adherence pre-treated with 100nM rapamycin (Calbiochem) over night (o/n), when indicated. LPS and Poly(I:C), used in final concentrations of 100ng/ml and 50μg/ml respectively, was purchased from Sigma.

Cells were placed on ice and washed with ice cold PBS. Lysis buffer was added and cells were scraped of with a rubber policeman. Lysates were transferred into clean eppendorf tube, incubated 10min on ice and frozen twice in liquid N_2 to complete lysis. Cellular debris was removed by 10min centrifugation at 1600g, 4 and protein concentrations were measure with 1:5 dilution of Bradford solution using a spectrophotometer. Concentrations were adjusted with lysis buffer and mixed with 4xSDS loading dye, heated for 5min at 95°C and stored at -80°C.

4.5.3 SDS page

Gel casting apparatus was assembled and well cleaned glass plates were filled with resolving gel (7,5% to 12%AA) whereas the gel edge was smoothed with isopropanol until polymerisation. Isopropanol was removed, Stacking gel added and the comb inserted. The fully polymerized gel was placed into electrophoresis chamber which was filled up with 1x Running buffer. The comb was removed and equal amounts of Lysates were loaded. As a marker, PageRuler TM prestained protein ladder (Fermentas, Thermo Scientific) was loaded into one of the slots. The SDS-PAGE was run at 70V until proteins started to seperate in the Seperation gel and run at 110V until the running front nearly reached the edge of the glass plates.

Stacking gel	**7.5%**	**10%**	**12%**	
1.33ml	2.5ml	3.33ml	4ml	30% Acrylamide (AA) solution
2.5ml	–	–	–	0.5M Tris-HCl pH6.8
–	2.5ml	2.5ml	2.5ml	1.5M Tris-HCl pH8.8
100μl	100μl	100μl	100μl	10% SDS
6.07ml	4.9ml	4.07ml	3.4ml	dH_2O
10μl	10μl	10μl	10μl	THEMED
100μl	100μl	100μl	100μl	10% APS

4.5.4 Wet blotting

The gel was assembled into a sandwich (sponge, 2 filter papers, gel, nitrocellulose membrane from peqlab, 2 filter papers, sponge) in a cassette, whereas each part was soaked in Harlow buffer before assembly. The cassette and an ice block was placed into Mini Trans-Blot Module (BIO-RAD) and the chamber was filled with ice cold Harlow buffer. Proteins were transferred at RT for 1h, 350mA.

4.5.5 Antibody staining and detection

The membrane was blocked for 1h at RT in TBST containing 4% milkpowder and washed 3x for 10min with TBST. The membrane was incubated with primary antibody (dissolved in TBST containing 5% BSA) o/n at 4°C. The next

day the membrane was washed trice as before and incubated with secondary antibody in TBST containing 4% milkpowder. 6). The membrane was washed again as before, was placed briefly in dH_2O and was then incubated with well mixed ECL detection reagent 1 and 2 (Thermo Scientific). Detection was carried with a Kodak Medical X-ray Processor 2000 (Kodak), whereas various exposure times were accessed and films were labeled and scanned.

Specificity	Label	Species	Dilution	Company	Catalog no
TSC2	none	rabbit	1:1000	Cell signaling	3612
p-Akt (S473)	none	rabbit	1:1000	Cell signaling	4060
p-S6 (S240/S244)	none	rabbit	1:3000	Cell signaling	2215
β-Tubulin	none	rabbit	1:5000	Cell signaling	2128
LIMP2	none	rabbit	1:1000	NovusBiol	NB400-129
TFEB	none	mouse	1:100	MyBiosource	MBS120432
p-p44/42	none	mouse	1:1000	Cell signaling	9106
p44/42	none	rabbit	1:1000	Cell signaling	9102
GAPDH	none	rabbit	1:25000	Trevigen	2275-PC-100
rabbit IgG	HRP	goat	1:10000	Bethyl	A120-101P
mouse IgG	HRP	goat	1:10000	Bethyl	A90-116P

4.6 Histology

4.6.1 Tissue preparation

Mouse tissues were fixed with 4% PFA at 4°C o/n, washed trice with 1xPBS and cut into smaller segments if necessary. The dehydration process was performed in four incubation steps (70% EtOH,90% EtOH, 100% EtOH and xylene; each 3x for 30min at RT) by a third party. Tissues were embedded in paraffin at 58°C using an automatic paraffin embedding system Histostar (Thermo Scientific). Blocks were cut into 5μm thick sections using a rotary automatic microtome (Thermo Scientific), mounted onto super-frost histological slides (Thermo Scientific) and dried o/n at RT.

Slides were heated for 15min at 60°C and after paraffin was dried assembled into cassettes (Thermo Scientific). Thereafter tissues were re-hydrated by an alcohol series — Xylene 10min, Xylene 10min, Isopropanol 5min, 96% EtOH 2min, 70% EtOH 2min, 50% EtOH 2min (all Thermo Scientific) and at least 5min in dH_2O) — as a preparation for both H&E and immunofluorescent staining.

4.6.2 H&E staining

Slides were stained for 2min with hematoxylin (Sigma-Aldrich) and washed under running tab water for 10 minutes. The above mentioned alcohol series

was started in reverse order — 50% EtOH 2min, 70% EtOH 2min — whereafter the slides were immersed in Eosin (Sigma-Aldrich) solution for 30sec - 1min and excess staining was removed for 30sec in 70% EtOH. Dehydration was continued with 96% EtOH for 2min and twice 5min Xylene, where after the slides were mounted with xylene based mounting medium (Thermo Scientific). Tissues were analyzed using a Axioskop microscope (Zeiss).

4.7 Immunofluorescent staining

Antigen retrieval was accessed by 20min autoclavation at 120°C in Citrate buffer (DAKO). Hereafter the slides were immobilized in disposable immunostaining chambers (Thermo Scientific) in dH_2O. After 3x washing with PBS, tissues were permeabilized with 0.1% TritonX in PBS and washed 3x with PBS. After blocking with 1% BSA in PBS for 20min primary antibodies and DAPI (1:1000; Roth) in PBS were added and incubated o/n at 4°C. The slides were washed 3x with PBS the next day and incubated with secondary antibodies, diluted in PBS, for 60min at RT. Then the slides were washed 3x with PBS and mounted with water base mounting medium (Thermo Scientific). Tissues were analyzed using a Axiophot fluorescent microscope (Zeiss).

Specificity	**Label**	**Species**	**Dilution**	**Company**	**Catalog no**
p-S6	none	rabbit	1:1000	Cell signaling	2215
MAC-2	Alexa488	rat	1:1000	Biolegend	125410
rabbit IgG	Alexa546	goat	1:10000	Invitrogen	A-11004

4.8 Electron microscopy

For transmission electron microscopy (TEM) 2-4x10^5 were seeded on sterile glass slides inserted in 12-well dishes, whereas the process of TEM was kindly performed by Clemens Röhrl using a Zeiss EM900 transmission electron microscope.

4.9 qPCR

4.9.1 RNA isolation

For qPCR 4-5x10^5 cells were seeded in 24-well plates in starvation media for 48h. BMDM were washed and resuspended in 500μl of Trizol (Ambion) and stored at -80°C until further usage. All further steps were performed on ice or at 4°C, otherwise specifically indicated. After 5min centrifugation at 13000rpm the trizol phase was transferred to a tube containing 120μl of ddH_2O and 100μl

of chloroform, and incubated for 10min on room temperature; the cell debris pellet was discarded. The solution was vortexed and centrifuged at 13000rpm for 15min and the aqueous phase was transferred into a fresh tube. Each sample was mixed with with 1μl Glycoblue (Ambion) and 280μl of cold isopropanol for mRNA precipitation. After 30min incubation, followed by 30min of centrifugation at 13000rpm, the supernatant was dicarded and mRNA pellets were washed 2x with 1 ml of 75% EtOH. The pellets were resuspended in Nuclease-free H_2O and concentrations were measure using a spectrophotometer.

4.9.2 cDNA synthesis

The cDNA synthesis was performed using GoScriptTM Reverse Transcription system (Promega, A5000). mRNA was adjusted to 300ng in 4μl, which was mixed with 1μl of random Primers and heated for 5 minutes at 75°C on a thermocycler (Peqlab). The samples were put on ice and immediately mixed with 15μl master mix. The program for the synthesis was set according to the guideline of the kit: 5min at 25°C; 60min at 42°C; 15min at 70°C and cooling to 4°C. The cDNA was diluted 1:11 in nuclease-free water and stored at -80°C.

Master Mix per sample
⋆ 7.3μl Nuclease-free H_2O
⋆ 4.0μl Goscript 5x reaction buffer
⋆ 1.2μl $MgCl_2$
⋆ 1.0μl 1PCR nucleotide mix
⋆ 0.5μl Recominant RNasin Ribonuclease inhibitor
⋆ 1.0μl Goscript reverse transcriptase

4.9.3 qRT-PCR

qRT-PCR was carried out using GoTaq Probe master mix (Promega). Whereas 2μl of cDNA and 8μl of master mix was used in each reaction. Duplicates were prepared on a 96-well plate (BIO- RAD), sealed with a transparent sealer (BIO-RAD) and plated into a miniOpticonTM real-time PCR detection system (BIO-RAD). The thermal cycle was set according to protocol: 2min at 95°C (polymerase activation),40 followed cycles including denaturation (15sec) and annealing/extension (1min). The raw data was analyzed with BIO-RAD CFX management program. The genes of interest include: LIMP2, HEXA, ATP6v1h. The expression levels of mRNA were normalized to the expression of beta-actin mRNA.

Master Mix per sample
⋆ 5.00μl 2x MasterMix
⋆ 0.02μl Forward- Primer
⋆ 0.02μl Reverse- Primer
⋆ 2.90μl Nuclease-free H_2O

4.10 *In vivo* treatment with everolimus

Mice were treated with 5mg/kg/day everolimus (Novartis pharma, AG) or with a placebo. The provided placebo was prepared as everolimus. Treatment was intragastrically administrated using a 30mm gavage needle (F.S.T).

Bibliography

[1] C. R. Sabin FR, Doan CA, "The discrimination of two types of phagocytic cells in the connective tissues by the supravital technique," *Contrib Embryol (Am)*, vol. 16, pp. 125–162, 1925.

[2] R. van Furth, Z. A. Cohn, J. G. Hirsch, J. H. Humphrey, W. G. Spector, and H. L. Langevoort, "The mononuclear phagocyte system: a new classification of macrophages, monocytes, and their precursor cells.," *Bull World Health Organ*, vol. 46, no. 6, pp. 845–852, 1972.

[3] K. Takahashi, "Development and differentiation of macrophages and related cells: Historical review and current concepts," *J Clin Exp Hematop*, vol. 41, no. 1, pp. 1–33, 2001.

[4] K. Takahashi, F. Yamamura, and M. Naito, "Differentiation, maturation, and proliferation of macrophages in the mouse yolk sac: a light-microscopic, enzyme-cytochemical, immunohistochemical, and ultrastructural study.," *J Leukoc Biol*, vol. 45, pp. 87–96, Feb 1989.

[5] G. Hoeffel, Y. Wang, M. Greter, P. See, P. Teo, B. Malleret, M. Leboeuf, D. Low, G. Oller, F. Almeida, S. H. Y. Choy, M. Grisotto, L. Renia, S. J. Conway, E. R. Stanley, J. K. Y. Chan, L. G. Ng, I. M. Samokhvalov, M. Merad, and F. Ginhoux, "Adult langerhans cells derive predominantly from embryonic fetal liver monocytes with a minor contribution of yolk sac-derived macrophages.," *J Exp Med*, vol. 209, pp. 1167–1181, Jun 2012.

[6] C. Schulz, E. Gomez Perdiguero, L. Chorro, H. Szabo-Rogers, N. Cagnard, K. Kierdorf, M. Prinz, B. Wu, S. E. W. Jacobsen, J. W. Pollard, J. Frampton, K. J. Liu, and F. Geissmann, "A lineage of myeloid cells independent of myb and hematopoietic stem cells.," *Science*, vol. 336, pp. 86–90, Apr 2012.

[7] E. L. Gautier, T. Shay, J. Miller, M. Greter, C. Jakubzick, S. Ivanov, J. Helft, A. Chow, K. G. Elpek, S. Gordonov, A. R. Mazloom, A. Ma'ayan, W.-J. Chua, T. H. Hansen, S. J. Turley, M. Merad, and G. J. Randolph, "Gene-expression profiles and transcriptional regulatory pathways that underlie the identity and diversity of mouse tissue macrophages.," *Nat Immunol*, vol. 13, pp. 1118–1128, Nov 2012.

[8] S. Yona, K.-W. Kim, Y. Wolf, A. Mildner, D. Varol, M. Breker, D. Strauss-Ayali, S. Viukov, M. Guilliams, A. Misharin, D. A. Hume, H. Perlman, B. Malissen, E. Zelzer, and S. Jung, "Fate mapping reveals origins and dynamics of monocytes and tissue macrophages under homeostasis.," *Immunity*, vol. 38, pp. 79–91, Jan 2013.

[9] L. C. Davies, S. J. Jenkins, J. E. Allen, and P. R. Taylor, "Tissue-resident macrophages.," *Nat Immunol*, vol. 14, pp. 986–995, Oct 2013.

[10] T. A. Wynn, A. Chawla, and J. W. Pollard, "Macrophage biology in development, homeostasis and disease.," *Nature*, vol. 496, pp. 445–455, Apr 2013.

[11] H. Yoshida, S. Hayashi, T. Kunisada, M. Ogawa, S. Nishikawa, H. Okamura, T. Sudo, L. D. Shultz, and S. Nishikawa, "The murine mutation osteopetrosis is in the coding region of the macrophage colony stimulating factor gene.," *Nature*, vol. 345, pp. 442–444, May 1990.

[12] X.-M. Dai, G. R. Ryan, A. J. Hapel, M. G. Dominguez, R. G. Russell, S. Kapp, V. Sylvestre, and E. R. Stanley, "Targeted disruption of the mouse colony-stimulating factor 1 receptor gene results in osteopetrosis, mononuclear phagocyte deficiency, increased primitive progenitor cell frequencies, and reproductive defects.," *Blood*, vol. 99, pp. 111–120, Jan 2002.

[13] Y. Wang, K. J. Szretter, W. Vermi, S. Gilfillan, C. Rossini, M. Cella, A. D. Barrow, M. S. Diamond, and M. Colonna, "Il-34 is a tissue-restricted ligand of csf1r required for the development of langerhans cells and microglia.," *Nat Immunol*, vol. 13, pp. 753–760, Aug 2012.

[14] M. Greter, I. Lelios, P. Pelczar, G. Hoeffel, J. Price, M. Leboeuf, T. M. Kundig, K. Frei, F. Ginhoux, M. Merad, and B. Becher, "Stroma-derived interleukin-34 controls the development and maintenance of langerhans cells and the maintenance of microglia.," *Immunity*, vol. 37, pp. 1050–1060, Dec 2012.

[15] M. Guilliams, I. De Kleer, S. Henri, S. Post, L. Vanhoutte, S. De Prijck, K. Deswarte, B. Malissen, H. Hammad, and B. N. Lambrecht, "Alveolar macrophages develop from fetal monocytes that differentiate into long-lived cells in the first week of life via gm-csf.," *J Exp Med*, vol. 210, pp. 1977–1992, Sep 2013.

[16] F. Geissmann, M. G. Manz, S. Jung, M. H. Sieweke, M. Merad, and K. Ley, "Development of monocytes, macrophages, and dendritic cells.," *Science*, vol. 327, pp. 656–661, Feb 2010.

[17] P. J. Murray and T. A. Wynn, "Protective and pathogenic functions of macrophage subsets.," *Nat Rev Immunol*, vol. 11, pp. 723–737, Nov 2011.

[18] S. Gordon, "Alternative activation of macrophages.," *Nat Rev Immunol*, vol. 3, pp. 23–35, Jan 2003.

[19] P. R. Taylor, L. Martinez-Pomares, M. Stacey, H.-H. Lin, G. D. Brown, and S. Gordon, "Macrophage receptors and immune recognition.," *Annu Rev Immunol*, vol. 23, pp. 901–944, 2005.

[20] T. Kawai and S. Akira, "The roles of tlrs, rlrs and nlrs in pathogen recognition.," *Int Immunol*, vol. 21, pp. 317–337, Apr 2009.

[21] A. Aderem and D. M. Underhill, "Mechanisms of phagocytosis in macrophages.," *Annu Rev Immunol*, vol. 17, pp. 593–623, 1999.

[22] O. V. Vieira, R. J. Botelho, and S. Grinstein, "Phagosome maturation: aging gracefully.," *Biochem J*, vol. 366, pp. 689–704, Sep 2002.

[23] J. W. Pollard, "Trophic macrophages in development and disease.," *Nat Rev Immunol*, vol. 9, pp. 259–270, Apr 2009.

[24] J. A. Chasis and N. Mohandas, "Erythroblastic islands: niches for erythropoiesis.," *Blood*, vol. 112, pp. 470–478, Aug 2008.

[25] A. Chow, M. Huggins, J. Ahmed, D. Hashimoto, D. Lucas, Y. Kunisaki, S. Pinho, M. Leboeuf, C. Noizat, N. van Rooijen, M. Tanaka, Z. J. Zhao, A. Bergman, M. Merad, and P. S. Frenette, "Cd169(+) macrophages provide a niche promoting erythropoiesis under homeostasis and stress.," *Nat Med*, vol. 19, pp. 429–436, Apr 2013.

[26] M. Kohyama, W. Ise, B. T. Edelson, P. R. Wilker, K. Hildner, C. Mejia, W. A. Frazier, T. L. Murphy, and K. M. Murphy, "Role for spi-c in the development of red pulp macrophages and splenic iron homeostasis.," *Nature*, vol. 457, pp. 318–321, Jan 2009.

[27] S. Wullschleger, R. Loewith, and M. N. Hall, "Tor signaling in growth and metabolism.," *Cell*, vol. 124, pp. 471–484, Feb 2006.

[28] Q. Yang and K.-L. Guan, "Expanding mtor signaling.," *Cell Res*, vol. 17, pp. 666–681, Aug 2007.

[29] M. Laplante and D. M. Sabatini, "mtor signaling in growth control and disease.," *Cell*, vol. 149, pp. 274–293, Apr 2012.

[30] D. Benjamin, M. Colombi, C. Moroni, and M. N. Hall, "Rapamycin passes the torch: a new generation of mtor inhibitors.," *Nat Rev Drug Discov*, vol. 10, pp. 868–880, Nov 2011.

[31] D.-H. Kim, D. D. Sarbassov, S. M. Ali, J. E. King, R. R. Latek, H. Erdjument-Bromage, P. Tempst, and D. M. Sabatini, "mtor interacts with raptor to form a nutrient-sensitive complex that signals to the cell growth machinery.," *Cell*, vol. 110, pp. 163–175, Jul 2002.

[32] E. Jacinto, R. Loewith, A. Schmidt, S. Lin, M. A. Ruegg, A. Hall, and M. N. Hall, "Mammalian tor complex 2 controls the actin cytoskeleton and is rapamycin insensitive.," *Nat Cell Biol*, vol. 6, pp. 1122–1128, Nov 2004.

[33] T. Kaizuka, T. Hara, N. Oshiro, U. Kikkawa, K. Yonezawa, K. Takehana, S.-I. Iemura, T. Natsume, and N. Mizushima, "Tti1 and tel2 are critical factors in mammalian target of rapamycin complex assembly.," *J Biol Chem*, vol. 285, pp. 20109–20116, Jun 2010.

[34] T. R. Peterson, M. Laplante, C. C. Thoreen, Y. Sancak, S. A. Kang, W. M. Kuehl, N. S. Gray, and D. M. Sabatini, "Deptor is an mtor inhibitor frequently overexpressed in multiple myeloma cells and required for their survival.," *Cell*, vol. 137, pp. 873–886, May 2009.

[35] E. Vander Haar, S.-I. Lee, S. Bandhakavi, T. J. Griffin, and D.-H. Kim, "Insulin signalling to mtor mediated by the akt/pkb substrate pras40.," *Nat Cell Biol*, vol. 9, pp. 316–323, Mar 2007.

[36] Y. Sancak, C. C. Thoreen, T. R. Peterson, R. A. Lindquist, S. A. Kang, E. Spooner, S. A. Carr, and D. M. Sabatini, "Pras40 is an insulin-regulated inhibitor of the mtorc1 protein kinase.," *Mol Cell*, vol. 25, pp. 903–915, Mar 2007.

[37] E. Jacinto, V. Facchinetti, D. Liu, N. Soto, S. Wei, S. Y. Jung, Q. Huang, J. Qin, and B. Su, "Sin1/mip1 maintains rictor-mtor complex integrity and regulates akt phosphorylation and substrate specificity.," *Cell*, vol. 127, pp. 125–137, Oct 2006.

[38] L. R. Pearce, X. Huang, J. Boudeau, R. Pawlowski, S. Wullschleger, M. Deak, A. F. M. Ibrahim, R. Gourlay, M. A. Magnuson, and D. R. Alessi, "Identification of protor as a novel rictor-binding component of mtor complex-2.," *Biochem J*, vol. 405, pp. 513–522, Aug 2007.

[39] J. D. Powell, K. N. Pollizzi, E. B. Heikamp, and M. R. Horton, "Regulation of immune responses by mtor.," *Annu Rev Immunol*, vol. 30, pp. 39–68, 2012.

[40] K. Katholnig, M. Linke, H. Pham, M. Hengstschlager, and T. Weichhart, "Immune responses of macrophages and dendritic cells regulated by mtor signalling.," *Biochem Soc Trans*, vol. 41, pp. 927–933, Aug 2013.

[41] P. Mellor, L. A. Furber, J. N. K. Nyarko, and D. H. Anderson, "Multiple roles for the p85alpha isoform in the regulation and function of pi3k signalling and receptor trafficking.," *Biochem J*, vol. 441, pp. 23–37, Jan 2012.

[42] E. J. McManus, B. J. Collins, P. R. Ashby, A. R. Prescott, V. Murray-Tait, L. J. Armit, J. S. C. Arthur, and D. R. Alessi, "The in vivo role of

ptdins(3,4,5)p3 binding to pdk1 ph domain defined by knockin mutation.," *EMBO J*, vol. 23, pp. 2071–2082, May 2004.

[43] D. D. Sarbassov, D. A. Guertin, S. M. Ali, and D. M. Sabatini, "Phosphorylation and regulation of akt/pkb by the rictor-mtor complex.," *Science*, vol. 307, pp. 1098–1101, Feb 2005.

[44] K. Inoki, Y. Li, T. Zhu, J. Wu, and K.-L. Guan, "Tsc2 is phosphorylated and inhibited by akt and suppresses mtor signalling.," *Nat Cell Biol*, vol. 4, pp. 648–657, Sep 2002.

[45] A. R. Tee, B. D. Manning, P. P. Roux, L. C. Cantley, and J. Blenis, "Tuberous sclerosis complex gene products, tuberin and hamartin, control mtor signaling by acting as a gtpase-activating protein complex toward rheb.," *Curr Biol*, vol. 13, pp. 1259–1268, Aug 2003.

[46] K. Inoki, Y. Li, T. Xu, and K.-L. Guan, "Rheb gtpase is a direct target of tsc2 gap activity and regulates mtor signaling.," *Genes Dev*, vol. 17, pp. 1829–1834, Aug 2003.

[47] P. P. Roux, B. A. Ballif, R. Anjum, S. P. Gygi, and J. Blenis, "Tumor-promoting phorbol esters and activated ras inactivate the tuberous sclerosis tumor suppressor complex via p90 ribosomal s6 kinase.," *Proc Natl Acad Sci U S A*, vol. 101, pp. 13489–13494, Sep 2004.

[48] L. Ma, Z. Chen, H. Erdjument-Bromage, P. Tempst, and P. P. Pandolfi, "Phosphorylation and functional inactivation of tsc2 by erk implications for tuberous sclerosis and cancer pathogenesis.," *Cell*, vol. 121, pp. 179–193, Apr 2005.

[49] K. Katholnig, C. C. Kaltenecker, H. Hayakawa, M. Rosner, C. Lassnig, G. J. Zlabinger, M. Gaestel, M. Muller, M. Hengstschlager, W. H. Horl, J. M. Park, M. D. Saemann, and T. Weichhart, "p38alpha senses environmental stress to control innate immune responses via mechanistic target of rapamycin.," *J Immunol*, vol. 190, pp. 1519–1527, Feb 2013.

[50] K. Inoki, H. Ouyang, T. Zhu, C. Lindvall, Y. Wang, X. Zhang, Q. Yang, C. Bennett, Y. Harada, K. Stankunas, C.-Y. Wang, X. He, O. A. MacDougald, M. You, B. O. Williams, and K.-L. Guan, "Tsc2 integrates wnt and energy signals via a coordinated phosphorylation by ampk and gsk3 to regulate cell growth.," *Cell*, vol. 126, pp. 955–968, Sep 2006.

[51] K. Inoki, T. Zhu, and K.-L. Guan, "Tsc2 mediates cellular energy response to control cell growth and survival.," *Cell*, vol. 115, pp. 577–590, Nov 2003.

[52] J. Brugarolas, K. Lei, R. Hurley, B. Manning, J. Reiling, E. Hafen, L. Witters, L. Ellisen, and W. J. Kaelin, "Regulation of mtor function in response to hypoxia by redd1 and the tsc1/tsc2 tumor suppressor complex.," *Genes Dev*, vol. 18, pp. 2893–2904, Dec 2004.

[53] X. M. Ma and J. Blenis, "Molecular mechanisms of mtor-mediated translational control.," *Nat Rev Mol Cell Biol*, vol. 10, pp. 307–318, May 2009.

[54] T. Haruta, T. Uno, J. Kawahara, A. Takano, K. Egawa, P. M. Sharma, J. M. Olefsky, and M. Kobayashi, "A rapamycin-sensitive pathway down-regulates insulin signaling via phosphorylation and proteasomal degradation of insulin receptor substrate-1.," *Mol Endocrinol*, vol. 14, pp. 783–794, Jun 2000.

[55] L. S. Harrington, G. M. Findlay, A. Gray, T. Tolkacheva, S. Wigfield, H. Rebholz, J. Barnett, N. R. Leslie, S. Cheng, P. R. Shepherd, I. Gout, C. P. Downes, and R. F. Lamb, "The tsc1-2 tumor suppressor controls insulin-pi3k signaling via regulation of irs proteins.," *J Cell Biol*, vol. 166, pp. 213–223, Jul 2004.

[56] K. Duvel, J. L. Yecies, S. Menon, P. Raman, A. I. Lipovsky, A. L. Souza, E. Triantafellow, Q. Ma, R. Gorski, S. Cleaver, M. G. Vander Heiden, J. P. MacKeigan, P. M. Finan, C. B. Clish, L. O. Murphy, and B. D. Manning, "Activation of a metabolic gene regulatory network downstream of mtor complex 1.," *Mol Cell*, vol. 39, pp. 171–183, Jul 2010.

[57] T. R. Peterson, S. S. Sengupta, T. E. Harris, A. E. Carmack, S. A. Kang, E. Balderas, D. A. Guertin, K. L. Madden, A. E. Carpenter, B. N. Finck, and D. M. Sabatini, "mtor complex 1 regulates lipin 1 localization to control the srebp pathway.," *Cell*, vol. 146, pp. 408–420, Aug 2011.

[58] J. T. Cunningham, J. T. Rodgers, D. H. Arlow, F. Vazquez, V. K. Mootha, and P. Puigserver, "mtor controls mitochondrial oxidative function through a yy1-pgc-1alpha transcriptional complex.," *Nature*, vol. 450, pp. 736–740, Nov 2007.

[59] A. L. Edinger and C. B. Thompson, "Akt maintains cell size and survival by increasing mtor-dependent nutrient uptake.," *Mol Biol Cell*, vol. 13, pp. 2276–2288, Jul 2002.

[60] M. M. Mihaylova and R. J. Shaw, "The ampk signalling pathway coordinates cell growth, autophagy and metabolism.," *Nat Cell Biol*, vol. 13, pp. 1016–1023, Sep 2011.

[61] Y. Sancak, T. R. Peterson, Y. D. Shaul, R. A. Lindquist, C. C. Thoreen, L. Bar-Peled, and D. M. Sabatini, "The rag gtpases bind raptor and mediate amino acid signaling to mtorc1.," *Science*, vol. 320, pp. 1496–1501, Jun 2008.

[62] Y. Sancak, L. Bar-Peled, R. Zoncu, A. L. Markhard, S. Nada, and D. M. Sabatini, "Ragulator-rag complex targets mtorc1 to the lysosomal surface and is necessary for its activation by amino acids.," *Cell*, vol. 141, pp. 290–303, Apr 2010.

[63] R. Zoncu, L. Bar-Peled, A. Efeyan, S. Wang, Y. Sancak, and D. M. Sabatini, "mtorc1 senses lysosomal amino acids through an inside-out mechanism that requires the vacuolar h(+)-atpase.," *Science*, vol. 334, pp. 678–683, Nov 2011.

[64] L. Bar-Peled, L. D. Schweitzer, R. Zoncu, and D. M. Sabatini, "Ragulator is a gef for the rag gtpases that signal amino acid levels to mtorc1.," *Cell*, vol. 150, pp. 1196–1208, Sep 2012.

[65] I. G. Ganley, D. H. Lam, J. Wang, X. Ding, S. Chen, and X. Jiang, "Ulk1.atg13.fip200 complex mediates mtor signaling and is essential for autophagy.," *J Biol Chem*, vol. 284, pp. 12297–12305, May 2009.

[66] N. Hosokawa, T. Hara, T. Kaizuka, C. Kishi, A. Takamura, Y. Miura, S.-i. Iemura, T. Natsume, K. Takehana, N. Yamada, J.-L. Guan, N. Oshiro, and N. Mizushima, "Nutrient-dependent mtorc1 association with the ulk1-atg13-fip200 complex required for autophagy.," *Mol Biol Cell*, vol. 20, pp. 1981–1991, Apr 2009.

[67] M. Sardiello, M. Palmieri, A. di Ronza, D. L. Medina, M. Valenza, V. A. Gennarino, C. Di Malta, F. Donaudy, V. Embrione, R. S. Polishchuk, S. Banfi, G. Parenti, E. Cattaneo, and A. Ballabio, "A gene network regulating lysosomal biogenesis and function.," *Science*, vol. 325, pp. 473–477, Jul 2009.

[68] C. Settembre, C. Di Malta, V. A. Polito, M. Garcia Arencibia, F. Vetrini, S. Erdin, S. U. Erdin, T. Huynh, D. Medina, P. Colella, M. Sardiello, D. C. Rubinsztein, and A. Ballabio, "Tfeb links autophagy to lysosomal biogenesis.," *Science*, vol. 332, pp. 1429–1433, Jun 2011.

[69] A. Roczniak-Ferguson, C. S. Petit, F. Froehlich, S. Qian, J. Ky, B. Angarola, T. C. Walther, and S. M. Ferguson, "The transcription factor tfeb links mtorc1 signaling to transcriptional control of lysosome homeostasis.," *Sci Signal*, vol. 5, p. ra42, Jun 2012.

[70] C. Settembre, R. Zoncu, D. L. Medina, F. Vetrini, S. Erdin, S. Erdin, T. Huynh, M. Ferron, G. Karsenty, M. C. Vellard, V. Facchinetti, D. M. Sabatini, and A. Ballabio, "A lysosome-to-nucleus signalling mechanism senses and regulates the lysosome via mtor and tfeb.," *EMBO J*, vol. 31, pp. 1095–1108, Mar 2012.

[71] J. A. Martina, Y. Chen, M. Gucek, and R. Puertollano, "Mtorc1 functions as a transcriptional regulator of autophagy by preventing nuclear transport of tfeb.," *Autophagy*, vol. 8, pp. 903–914, Jun 2012.

[72] C. de Duve, "The lysosome turns fifty.," *Nat Cell Biol*, vol. 7, pp. 847–849, Sep 2005.

[73] J. Berthet, L. Berthet, F. Appelmans, and C. de Duve, "Tissue fractionation studies. ii. the nature of the linkage between acid phosphatase and mitochondria in rat-liver tissue.," *Biochem J*, vol. 50, pp. 182–189, Dec 1951.

[74] C. DE DUVE, B. C. PRESSMAN, R. GIANETTO, R. WATTIAUX, and F. APPELMANS, "Tissue fractionation studies. 6. intracellular distribution patterns of enzymes in rat-liver tissue.," *Biochem J*, vol. 60, pp. 604–617, Aug 1955.

[75] C. Settembre, A. Fraldi, D. L. Medina, and A. Ballabio, "Signals from the lysosome: a control centre for cellular clearance and energy metabolism.," *Nat Rev Mol Cell Biol*, vol. 14, pp. 283–296, May 2013.

[76] J. P. Luzio, P. R. Pryor, and N. A. Bright, "Lysosomes: fusion and function.," *Nat Rev Mol Cell Biol*, vol. 8, pp. 622–632, Aug 2007.

[77] P. Saftig and J. Klumperman, "Lysosome biogenesis and lysosomal membrane proteins: trafficking meets function.," *Nat Rev Mol Cell Biol*, vol. 10, pp. 623–635, Sep 2009.

[78] B. A. Schroder, C. Wrocklage, A. Hasilik, and P. Saftig, "The proteome of lysosomes.," *Proteomics*, vol. 10, pp. 4053–4076, Nov 2010.

[79] H. Schulze, T. Kolter, and K. Sandhoff, "Principles of lysosomal membrane degradation: Cellular topology and biochemistry of lysosomal lipid degradation.," *Biochim Biophys Acta*, vol. 1793, pp. 674–683, Apr 2009.

[80] C. J. Galloway, G. E. Dean, M. Marsh, G. Rudnick, and I. Mellman, "Acidification of macrophage and fibroblast endocytic vesicles in vitro.," *Proc Natl Acad Sci U S A*, vol. 80, pp. 3334–3338, Jun 1983.

[81] V. Marshansky and M. Futai, "The v-type h+-atpase in vesicular trafficking: targeting, regulation and function.," *Curr Opin Cell Biol*, vol. 20, pp. 415–426, Aug 2008.

[82] J. A. Mindell, "Lysosomal acidification mechanisms.," *Annu Rev Physiol*, vol. 74, pp. 69–86, 2012.

[83] S. Ohkuma, Y. Moriyama, and T. Takano, "Identification and characterization of a proton pump on lysosomes by fluorescein-isothiocyanate-dextran fluorescence.," *Proc Natl Acad Sci U S A*, vol. 79, pp. 2758–2762, May 1982.

[84] M. L. Schultz, L. Tecedor, M. Chang, and B. L. Davidson, "Clarifying lysosomal storage diseases.," *Trends Neurosci*, vol. 34, pp. 401–410, Aug 2011.

[85] F. Henell, J. L. Ericsson, and H. Glaumann, "Degradation of phagocytosed lysosomes by kupffer cell lysosomes.," *Lab Invest*, vol. 48, pp. 556–564, May 1983.

[86] W. F. Neiss, "A coat of glycoconjugates on the inner surface of the lysosomal membrane in the rat kidney.," *Histochemistry*, vol. 80, no. 6, pp. 603–608, 1984.

[87] K. Olden, B. A. Bernard, Y. T.-K. Humphries, M J, S. L. Yeo, K-T ans White, S. A. Newton, H. C. Bauer, and J. B. Parent, "Function of glycoprotein glycans.," *Trends Biochem. Sci.*, vol. 10, pp. 78—82, Feb 1985.

[88] D. M. Fambrough, K. Takeyasu, J. Lippincott-Schwarz, and N. R. Siegel, "Structure of lep100, a glycoprotein that shuttles between lysosomes and the plasma membrane, deduced from the nucleotide sequence of the encoding cdna.," *J Cell Biol*, vol. 106, pp. 61–67, Jan 1988.

[89] B. L. Granger, S. A. Green, C. A. Gabel, C. L. Howe, I. Mellman, and A. Helenius, "Characterization and cloning of lgp110, a lysosomal membrane glycoprotein from mouse and rat cells.," *J Biol Chem*, vol. 265, pp. 12036–12043, Jul 1990.

[90] R. Kundra and S. Kornfeld, "Asparagine-linked oligosaccharides protect lamp-1 and lamp-2 from intracellular proteolysis.," *J Biol Chem*, vol. 274, pp. 31039–31046, Oct 1999.

[91] F. M. Platt, B. Boland, and A. C. van der Spoel, "The cell biology of disease: lysosomal storage disorders: the cellular impact of lysosomal dysfunction.," *J Cell Biol*, vol. 199, pp. 723–734, Nov 2012.

[92] H. Appelqvist, P. Waster, K. Kagedal, and K. Ollinger, "The lysosome: from waste bag to potential therapeutic target.," *J Mol Cell Biol*, vol. 5, pp. 214–226, Aug 2013.

[93] G. J. Doherty and H. T. McMahon, "Mechanisms of endocytosis.," *Annu Rev Biochem*, vol. 78, pp. 857–902, 2009.

[94] S. Kumari, S. Mg, and S. Mayor, "Endocytosis unplugged: multiple ways to enter the cell.," *Cell Res*, vol. 20, pp. 256–275, Mar 2010.

[95] M. Bohdanowicz and S. Grinstein, "Role of phospholipids in endocytosis, phagocytosis, and macropinocytosis.," *Physiol Rev*, vol. 93, pp. 69–106, Jan 2013.

[96] S. Sigismund, T. Woelk, C. Puri, E. Maspero, C. Tacchetti, P. Transidico, P. P. Di Fiore, and S. Polo, "Clathrin-independent endocytosis of ubiquitinated cargos.," *Proc Natl Acad Sci U S A*, vol. 102, pp. 2760–2765, Feb 2005.

[97] S. Sigismund, E. Argenzio, D. Tosoni, E. Cavallaro, S. Polo, and P. P. Di Fiore, "Clathrin-mediated internalization is essential for sustained egfr signaling but dispensable for degradation.," *Dev Cell*, vol. 15, pp. 209–219, Aug 2008.

[98] A. De Donatis, G. Comito, F. Buricchi, M. C. Vinci, A. Parenti, A. Caselli, G. Camici, G. Manao, G. Ramponi, and P. Cirri, "Proliferation versus migration in platelet-derived growth factor signaling: the key role of endocytosis.," *J Biol Chem*, vol. 283, pp. 19948–19956, Jul 2008.

[99] J. L. Goldstein and M. S. Brown, "The ldl receptor.," *Arterioscler Thromb Vasc Biol*, vol. 29, pp. 431–438, Apr 2009.

[100] J. Rink, E. Ghigo, Y. Kalaidzidis, and M. Zerial, "Rab conversion as a mechanism of progression from early to late endosomes.," *Cell*, vol. 122, pp. 735–749, Sep 2005.

[101] S. Lefrancois, J. Zeng, A. J. Hassan, M. Canuel, and C. R. Morales, "The lysosomal trafficking of sphingolipid activator proteins (saps) is mediated by sortilin.," *EMBO J*, vol. 22, pp. 6430–6437, Dec 2003.

[102] D. Reczek, M. Schwake, J. Schroder, H. Hughes, J. Blanz, X. Jin, W. Brondyk, S. Van Patten, T. Edmunds, and P. Saftig, "Limp-2 is a receptor for lysosomal mannose-6-phosphate-independent targeting of beta-glucocerebrosidase.," *Cell*, vol. 131, pp. 770–783, Nov 2007.

[103] O. Hernandez, S. Way, J. r. McKenna, and M. J. Gambello, "Generation of a conditional disruption of the tsc2 gene.," *Genesis*, vol. 45, pp. 101–106, Feb 2007.

[104] B. E. Clausen, C. Burkhardt, W. Reith, R. Renkawitz, and I. Forster, "Conditional gene targeting in macrophages and granulocytes using lysmcre mice.," *Transgenic Res*, vol. 8, pp. 265–277, Aug 1999.

[105] S. Pena-Llopis, S. Vega-Rubin-de Celis, J. C. Schwartz, N. C. Wolff, T. A. T. Tran, L. Zou, X.-J. Xie, D. R. Corey, and J. Brugarolas, "Regulation of tfeb and v-atpases by mtorc1.," *EMBO J*, vol. 30, pp. 3242–3258, Aug 2011.

[106] J. L. Goldstein, G. Y. Brunschede, and M. S. Brown, "Inhibition of proteolytic degradation of low density lipoprotein in human fibroblasts by chloroquine, concanavalin a, and triton wr 1339.," *J Biol Chem*, vol. 250, pp. 7854–7862, Oct 1975.

[107] S.-D. Ha, B. Ham, J. Mogridge, P. Saftig, S. Lin, and S. O. Kim, "Cathepsin b-mediated autophagy flux facilitates the anthrax toxin receptor 2-mediated delivery of anthrax lethal factor into the cytoplasm.," *J Biol Chem*, vol. 285, pp. 2120–2129, Jan 2010.

[108] T. Ganz, "Macrophages and systemic iron homeostasis.," *J Innate Immun*, vol. 4, no. 5-6, pp. 446–453, 2012.

[109] K. Araki, A. H. Ellebedy, and R. Ahmed, "Tor in the immune system.," *Curr Opin Cell Biol*, vol. 23, pp. 707–715, Dec 2011.

[110] H. Yang, X. Wang, Y. Zhang, H. Liu, J. Liao, K. Shao, Y. Chu, and G. Liu, "Modulation of tsc-mtor signaling on immune cells in immunity and autoimmunity.," *J Cell Physiol*, vol. 229, pp. 17–26, Jan 2014.

[111] T. Weichhart, G. Costantino, M. Poglitsch, M. Rosner, M. Zeyda, K. M. Stuhlmeier, T. Kolbe, T. M. Stulnig, W. H. Horl, M. Hengstschlager, M. Muller, and M. D. Saemann, "The tsc-mtor signaling pathway regulates the innate inflammatory response.," *Immunity*, vol. 29, pp. 565–577, Oct 2008.

[112] H. Pan, T. F. O'Brien, P. Zhang, and X.-P. Zhong, "The role of tuberous sclerosis complex 1 in regulating innate immunity.," *J Immunol*, vol. 188, pp. 3658–3666, Apr 2012.

[113] V. Byles, A. J. Covarrubias, I. Ben-Sahra, D. W. Lamming, D. M. Sabatini, B. D. Manning, and T. Horng, "The tsc-mtor pathway regulates macrophage polarization.," *Nat Commun*, vol. 4, p. 2834, 2013.

[114] S. Sarkar, "Regulation of autophagy by mtor-dependent and mtor-independent pathways: autophagy dysfunction in neurodegenerative diseases and therapeutic application of autophagy enhancers.," *Biochem Soc Trans*, vol. 41, pp. 1103–1130, Oct 2013.

[115] Y.-H. Hung, L. M.-W. Chen, J.-Y. Yang, and W. Y. Yang, "Spatiotemporally controlled induction of autophagy-mediated lysosome turnover.," *Nat Commun*, vol. 4, p. 2111, 2013.

[116] G. H. Xiao, F. Shoarinejad, F. Jin, E. A. Golemis, and R. S. Yeung, "The tuberous sclerosis 2 gene product, tuberin, functions as a rab5 gtpase activating protein (gap) in modulating endocytosis.," *J Biol Chem*, vol. 272, pp. 6097–6100, Mar 1997.

[117] D. Cox, D. J. Lee, B. M. Dale, J. Calafat, and S. Greenberg, "A rab11-containing rapidly recycling compartment in macrophages that promotes phagocytosis.," *Proc Natl Acad Sci U S A*, vol. 97, pp. 680–685, Jan 2000.

[118] Y. Ohsaki, M. Suzuki, Y. Shinohara, and T. Fujimoto, "Lysosomal accumulation of mtor is enhanced by rapamycin.," *Histochem Cell Biol*, vol. 134, pp. 537–544, Dec 2010.

[119] J. Zhou, S.-H. Tan, V. Nicolas, C. Bauvy, N.-D. Yang, J. Zhang, Y. Xue, P. Codogno, and H.-M. Shen, "Activation of lysosomal function in the course of autophagy via mtorc1 suppression and autophagosome-lysosome fusion.," *Cell Res*, vol. 23, pp. 508–523, Apr 2013.

[120] U. Kornak, E. Reynders, A. Dimopoulou, J. van Reeuwijk, B. Fischer, A. Rajab, B. Budde, P. Nurnberg, F. Foulquier, D. Lefeber, Z. Urban, S. Gruenewald, W. Annaert, H. G. Brunner, H. van Bokhoven, R. Wevers, E. Morava, G. Matthijs, L. Van Maldergem, and S. Mundlos, "Impaired

glycosylation and cutis laxa caused by mutations in the vesicular h+-atpase subunit atp6v0a2.," *Nat Genet*, vol. 40, pp. 32–34, Jan 2008.

[121] I. Nakamura, N. Takahashi, T. Sasaki, S. Tanaka, N. Udagawa, H. Murakami, K. Kimura, Y. Kabuyama, T. Kurokawa, and T. Suda, "Wortmannin, a specific inhibitor of phosphatidylinositol-3 kinase, blocks osteoclastic bone resorption.," *FEBS Lett*, vol. 361, pp. 79–84, Mar 1995.

[122] I. Nakamura, T. Sasaki, S. Tanaka, N. Takahashi, E. Jimi, T. Kurokawa, Y. Kita, S. Ihara, T. Suda, and Y. Fukui, "Phosphatidylinositol-3 kinase is involved in ruffled border formation in osteoclasts.," *J Cell Physiol*, vol. 172, pp. 230–239, Aug 1997.

[123] M. Lu, Y. Y. Sautin, L. S. Holliday, and S. L. Gluck, "The glycolytic enzyme aldolase mediates assembly, expression, and activity of vacuolar h+-atpase.," *J Biol Chem*, vol. 279, pp. 8732–8739, Mar 2004.

[124] Y. Y. Sautin, M. Lu, A. Gaugler, L. Zhang, and S. L. Gluck, "Phosphatidylinositol 3-kinase-mediated effects of glucose on vacuolar h+-atpase assembly, translocation, and acidification of intracellular compartments in renal epithelial cells.," *Mol Cell Biol*, vol. 25, pp. 575–589, Jan 2005.

[125] L. Yu, C. K. McPhee, L. Zheng, G. A. Mardones, Y. Rong, J. Peng, N. Mi, Y. Zhao, Z. Liu, F. Wan, D. W. Hailey, V. Oorschot, J. Klumperman, E. H. Baehrecke, and M. J. Lenardo, "Termination of autophagy and reformation of lysosomes regulated by mtor.," *Nature*, vol. 465, pp. 942–946, Jun 2010.

[126] Y. Rong, M. Liu, L. Ma, W. Du, H. Zhang, Y. Tian, Z. Cao, Y. Li, H. Ren, C. Zhang, L. Li, S. Chen, J. Xi, and L. Yu, "Clathrin and phosphatidylinositol-4,5-bisphosphate regulate autophagic lysosome reformation.," *Nat Cell Biol*, vol. 14, pp. 924–934, Sep 2012.

[127] J. A. Martina and R. Puertollano, "Rag gtpases mediate amino acid-dependent recruitment of tfeb and mitf to lysosomes.," *J Cell Biol*, vol. 200, pp. 475–491, Feb 2013.

[128] B. M. Wiczer and G. Thomas, "Phospholipase d and mtorc1: nutrients are what bring them together.," *Sci Signal*, vol. 5, p. pe13, Mar 2012.

[129] N. Martinez-Lopez, D. Athonvarangkul, P. Mishall, S. Sahu, and R. Singh, "Autophagy proteins regulate erk phosphorylation.," *Nat Commun*, vol. 4, p. 2799, 2013.

[130] B. Ravikumar, S. Imarisio, S. Sarkar, C. J. O'Kane, and D. C. Rubinsztein, "Rab5 modulates aggregation and toxicity of mutant huntingtin through macroautophagy in cell and fly models of huntington disease.," *J Cell Sci*, vol. 121, pp. 1649–1660, May 2008.

[131] Z. Dou, J.-A. Pan, H. A. Dbouk, L. M. Ballou, J. L. DeLeon, Y. Fan, J.-S. Chen, Z. Liang, G. Li, J. M. Backer, R. Z. Lin, and W.-X. Zong, "Class ia pi3k p110beta subunit promotes autophagy through rab5 small gtpase in response to growth factor limitation.," *Mol Cell*, vol. 50, pp. 29–42, Apr 2013.

[132] S. R. Greenhill and D. N. Kotton, "Pulmonary alveolar proteinosis: a bench-to-bedside story of granulocyte-macrophage colony-stimulating factor dysfunction.," *Chest*, vol. 136, pp. 571–577, Aug 2009.

[133] G. A. Grabowski, "Gaucher disease and other storage disorders.," *Hematology Am Soc Hematol Educ Program*, vol. 2012, pp. 13–18, 2012.

[134] C.-L. Hsu, W. Lin, D. Seshasayee, Y.-H. Chen, X. Ding, Z. Lin, E. Suto, Z. Huang, W. P. Lee, H. Park, M. Xu, M. Sun, L. Rangell, J. L. Lutman, S. Ulufatu, E. Stefanich, C. Chalouni, M. Sagolla, L. Diehl, P. Fielder, B. Dean, M. Balazs, and F. Martin, "Equilibrative nucleoside transporter 3 deficiency perturbs lysosome function and macrophage homeostasis.," *Science*, vol. 335, pp. 89–92, Jan 2012.

[135] R. M. Yates, A. Hermetter, G. A. Taylor, and D. G. Russell, "Macrophage activation downregulates the degradative capacity of the phagosome.," *Traffic*, vol. 8, pp. 241–250, Mar 2007.

[136] A. Savina, C. Jancic, S. Hugues, P. Guermonprez, P. Vargas, I. C. Moura, A.-M. Lennon-Dumenil, M. C. Seabra, G. Raposo, and S. Amigorena, "Nox2 controls phagosomal ph to regulate antigen processing during crosspresentation by dendritic cells.," *Cell*, vol. 126, pp. 205–218, Jul 2006.

A. Abstract

Macrophages are professional phagocytes whose various immunologic effector-functions are directed by multiple signaling cascades. Growth factors, nutrients and also TLR-ligands activate the PI3K-TSC1/2-mTORC1 pathway. Thus, the suppressive function of TSC1/2 is released, whereupon mTORC1 becomes activated. This thesis is focused on the characterization of a mouse model that harbors a conditional knock-out of TSC2 in macrophages and granulocytes ($TSC2^{\Delta M}$). We found enhanced mitochondrial metabolism in $TSC2^{\Delta M}$ macrophages while their lysosomes were compromised. Constitutive mTORC1 signaling elevated endocytic uptake and lysosomal pH, and rendered $TSC2^{\Delta M}$ macrophages unable to degrade the lysosomal substrate LDL. It has been shown recently that active mTORC1 is spaciotemporally linked to the lysosome and that it negatively regulates TFEB, which drives the expression of autophagic and lysosomal genes. The lysosome degrades cellular organelles and molecules into their building blocks, and consequently plays a fundamental role in efficient phagocyte functions. Interestingly, TFEB was transcriptional active (non-phosphorylated) despite mTORC1 activity, suggesting the involvement of another TFEB-regulating kinase. ERK, which has previously been shown to target TFEB, was identified as a possible candidate. Accumulation of hypertrophic macrophages in various organs is a common feature of some lysosomal storage diseases. $TSC2^{\Delta M}$ mice displayed a comparable phenotype, and we also found signs of perturbed splenic erythro-phagocytosis. Treatment with an mTORC1-specific inhibitor rescued and/or prevented these manifestations. These findings highlight the role of mTORC1-signaling in macrophages on their behavior/functions in vivo and their lysosomal and mitochondrial capacity and represent a novel aspect of mTORC1-mediated macrophage modulation.

B. Zusammenfassung

Makrophagen sind professionelle Phagozyten, deren immunologische Funktionen von diversen Signalwegen reguliert werden. Neben Wachstumsfaktoren und Nährstoffen aktivieren auch TLR-Liganden die PI3K-TSC1/2-mTORC1 Kaskade, wodurch die inhibitorische Wirkung von TSC1/2 aufgehoben und mTORC1 aktiviert wird. Während dieser Masterarbeit wurde ein Mausmodell mit einem Makrophagen- und Granolozyten-spezifischen TSC2 Knock-out ($TSC2^{\Delta M}$) charakterisiert. $TSC2^{\Delta M}$ Makrophagen zeigten verstärkten mitochondrialen Metabolismus, aber ihre Lysosomen waren nur beschränkt funktionell. Anhaltende mTORC1 Aktivität verstärkte die endozytische Aufnahme und erhöhte den lysosomalen pH. Weiters konnten $TSC2^{\Delta M}$ Makrophagen das lysosomale Substrat LDL nicht abbauen. Es wurde erst kürzlich gezeigt, dass mTORC1 den Transkriptionsfaktor TFEB negativ reguliert, welcher die Transkription von lysosomalen und autophagischen Genen induziert. Lysosomen verdauen zelluläre Organellen und Makromoleküle, weshalb diese Organellen eine zentrale Rolle in der Funktion von phagozytierenden Zellen spielen. Zu unserer Überraschung war TFEB - trotz erhöhter mTORC1 Aktivität - in $TSC2^{\Delta M}$ Makrophagen nicht phosphoryliert, was auf eine zusätzliche TFEB-regulierende Kinase hinwies. ERK, welches schon als Regulator von TFEB beschrieben ist, wurde als möglicher Kandidat identifiziert. In manchen lysosomalen Speicherkrankheiten akkumulieren hypertrophische Makrophagen in diversen Organen. Dies war auch in $TSC2^{\Delta M}$ Mäusen zu beobachten, was besonders die Alveolarstruktur der Lunge beeinträchtigte. Ausserdem war die Erythrozyten-Phagozytose in der Milz von $TSC2^{\Delta M}$ Mäusen vermindert. Behandlung der Mäuse mit einem mTORC1-Inhibitor normalisierte den Phänotyp. Diese Ergebnisse zeigen, dass die Aktivität von mTORC1 in Makrophagen den mitochondrialen und lysososomalen Metabolismus und weiters dessen Verhalten/Funktion in vivo beeinflusst und repräsentieren einen neuen Aspekt des mTOR-Pathway in Makrophagen.

C. Curriculum Vitae

Personal Data

Name:	Monika Linke
Date of birth:	7^{th} of March, 1986
Place of birth:	Gänserdorf, Lower Austria
Nationality:	Austrian

Scientific education

10/2007 - 10/2011	**Bachelor Studies**, ,,Microbiology and Genetics" **University of Vienna**
10/2010 - 12/2010	**Bachelor Thesis**, P. Kovarik Lab, Max F. Perutz Laboratories, Vienna *,,Chromatin-binding as a need for tyrosine dephosphorylation of IFN-γ-activated transcription factor Stat1."*
10/2011 - ongoing	**Master Studies**, ,,Microbiology and Immunobiology" **University of Vienna**
07/2012 - 02/2014	**Master Thesis**, T. Weichhart Lab, Institute of Medical Genetics, Vienna *,,The function of TSC2 in macrophages in regard to tissue homeostasis and metabolism."*

Publications

K. Katholnig, M. Linke, H. Pham, M. Hengstschlager, and T. Weichhart, ,,Immune responses of macrophages and dendritic cells regulated by mtor signalling.," *Biochem Soc Trans*, vol. 41, pp. 927933, Aug 2013.

D. Acknowledgments

First I would like to thank Thomas Weichhart for his scientific and mentoring endeavor. It was and is a marvelous challenge to work on this project and I sincerely appreciate the opportunity. Mario Mikula and his lab gave generous support in histologic staining, as did Birgit Niederreiter who performed immunohistology of feet tissue. I also would like to express my gratitude to the group around Herbert Stangl for their technical expertise regarding lysosomal assays and Clemens Röhrl for the performance of the electron microscopy. Many thanks to the people in the lab past and present. I especially am thankful to Ha Pham and Margit Rosner, who have been extremely helpful in fixing problems and who picked me up when my scope was down. It is a privilege, and a lot of fun, to work near such excellent scientists. Last but not least, I want to thank my boyfriend, my big crazy family and my friends for their continuous support despite my working hours and my incomprehensible scientific stories... - I sincerely appreciate it!!